The Zhenya Mammoth (Mammuthus primigenius (Blum.)): Taphonomy, geology, age, morphology and ancient DNA of a 48,000 year old frozen mummy from western Taimyr, Russia

Maschenko, Evgeny N.; Potapova, Olga R.; Vershinina, Alisa; Shapiro, Beth; Streletskaya, Irina D.; Vasiliev, Alexander A.; Oblogov, Gleb E.; Kharlamova, Anastasia S.; Potapov, Eugene; van der Plicht, J.

Published in:
Quaternary International

DOI:
10.1016/j.quaint.2017.06.055

Publication date:
2017

Quaternary International 445 (2017) 104–134

Contents lists available at ScienceDirect

Quaternary International

journal homepage: www.elsevier.com/locate/quaint

The Zhenya Mammoth (*Mammuthus primigenius* (Blum.)): Taphonomy, geology, age, morphology and ancient DNA of a 48,000 year old frozen mummy from western Taimyr, Russia

Evgeny N. Maschenko [a], Olga R. Potapova [b, *], Alisa Vershinina [c], Beth Shapiro [d], Irina D. Streletskaya [e], Alexander A. Vasiliev [f], Gleb E. Oblogov [f], Anastasia S. Kharlamova [g], Eugene Potapov [h], J. van der Plicht [i], Alexey N. Tikhonov [j], Natalia V. Serdyuk [a], Konstantin K. Tarasenko [a]

[a] *Borissiak Paleontological Institute, Russian Academy of the Sciences (PIN RAS), 123 Profsoyuznaia, 117 997 Moscow, Russia*
[b] *Mammoth Site of Hot Springs, SD., Inc., 1800 Hwy 18 Bypass, Hot Springs, SD 57747, USA*
[c] *Department of Ecology and Evolutionary Biology, University of California, Santa Cruz, CA 95064, USA*
[d] *Department of Ecology and Evolutionary Biology & Santa Cruz Genomics Institute, University of California, Santa Cruz, CA 95064, USA*
[e] *Lomonosov Moscow State University (MSU), Department of Geography, Leninskie Gory, Moscow 119991, Russia*
[f] *Institute of the Earth Cryosphere, Siberian Branch of Russian Academy of Sciences (SB RAS), 36 Malygina, Tyumen 625000, Russia; University of Tyumen, Volodarskogo ul., 3; 625003 Tyumen, Russia*
[g] *Research Institute of Human Morphology, 3 Tsurupy, Moscow 117418, Russia*
[h] *Bryn Athyn College, College Drive, Bryn Athyn, PA 19009, USA*
[i] *Center for Isotope Research, University of Groningen, 712 CP Groningen, The Netherlands*
[j] *Zoological Institute, Russian Academy of Sciences (ZIN RAS), 1 Universitetskaya Nabereznaia, St. Petersburg 119 034, Russia*

ARTICLE INFO

Article history:
Received 29 February 2016
Received in revised form
24 May 2017
Accepted 21 June 2017
Available online 12 August 2017

Keywords:
Woolly Mammoth
Haplogroup
Pathology
Pleistocene
Siberia

ABSTRACT

This paper reports the results of an in-depth analysis of the frozen remains of a woolly mammoth (*Mammuthus primigenius*) named Zhenya, which has been dated to 48,000 cal BP. The carcass, found near the mouth of the Yenisey River in eastern Siberia, was a juvenile male whose ontogenetic age at death was 8–10 AEY. Its reconstructed live height at the shoulders (pSH 227.4 cm) was the equal of some adult female woolly mammoths and extant elephants. The large stature and a flaked off tusk tip that matches breaks on tusks of male African elephants are indirect indications that this mammoth most likely had reached sexual maturity, had been expelled from its maternal herd, and had been in at least one fight with another male.

The mammoth's bones were relatively healthy, although some had minor lesions. Rudimentary upper second molars (M2/m2) were present, but no lower second molars were found in the alveoli, and the left tusk had never developed. Despite the abnormal development of the upper and lower second molars, the cheek teeth which were in wear (Dp4/dp4 and M1/m1) showed normal function without any indications of developmental delay.

The completed growth of the light-colored dentin bands on the tusk strongly suggests the Fall of the year was the season of death. This season is also supported by accumulated fat in the upper parts of the torso, indicative of physiological preparation for the winter ahead. The few minor traces of carnivore scavenging, the little disturbed condition of the carcass, and the absence of bone modifications made by human actions, along with the social status of this young male animal, are interpreted here as highly probable evidence that the Zhenya Mammoth died from unrecoverable injuries inflicted during a bull-to-bull fight.

Abbreviations: PIN, Borissiak Paleontological Institute; Russian Academy of the Sciences, Moscow; Russia, ZIN; Zoological Institute, Russian Academy of Sciences; St. Petersburg, Russia.

* Corresponding author.
E-mail address: olgap@mammothsite.org (O.R. Potapova).

http://dx.doi.org/10.1016/j.quaint.2017.06.055

The mineralogical analysis of site sediments revealed that the mammoth's burial *in situ* took place in the Yenisey River valley seasonally inundated by the river, which together with Fall's freezing temperatures protected the carcass from scavengers. An analysis of ancient DNA provides strong support for Zhenya's mitochondrial lineage within the deeply diverging clade III haplogroup B.

1. Introduction

This paper summarizes the results of studies made on the well preserved frozen remains of a woolly mammoth (*Mammuthus primigenius*) which was recently discovered near the mouth of the Yenisei River in arctic Siberia. The significance of this find is exceptional because of its completeness and good preservation.

The woolly mammoth, *Mammuthus primigenius* (Blumenbach, 1799), has been studied for over 200 years (Cuvier, 1799; Blumenbach, 1799; Garutt, 2001). Of fundamental importance are the discoveries and studies of frozen corpses found in Siberia, which have provided valuable data on anatomy, physiology, diet, ecology, biology, parasites, and causes of death (Zalenskii, 1903; Maschenko, 2002; van Geel et al., 2011; Fisher et al., 2012; Rountrey et al., 2012; Maschenko et al., 2013; Fisher et al., 2014; Glamazdin et al., 2014a, b).

The northern territories of Western Siberia, particularly the Yamal, Gydan, and Taimyr Peninsulas, are known for several major mammoth discoveries. Among them was the first find of a woolly mammoth carcass ever reported from Siberia (Lower Yenisey River) by Ysbrand Ides in 1692, which was sent by Tsar Peter the Great to China (Tolmachoff, 1929). About three centuries later discoveries of frozen woolly mammoth corpses and skeletons became more common in this region. These discoveries included two baby mammoths, nicknamed Masha and Lyuba (Vereschagin, 1999; Kuzmina, 1999; Fisher et al., 2012), the adolescent (10–12 year old) Yuribei Mammoth (Dubrovo, 1982), and a few adults. Among the adults are skeletons of the neotype individual of *M. primigenius* (the Taimyr Mammoth) (Garutt and Dubinin, 1951; Garutt et al., 1990), the Trofimov Mammoth, the Kutomanov Mammoth (Averianov, 1994), and the Kastatyakh Mammoth (Kirillova et al., 2011).

The mammoth find reported here has been named the Zhenya Mammoth (Fig. 1), and it is the most complete skeleton of a woolly mammoth presently known (Maschenko et al., 2014a, b; Maschenko et al., 2015). It also has been claimed to bear marks on the bones indicative of human activity (Pitulko et al., 2016); a detailed geological description and analysis of the Zhenya Mammoth site, the methods of excavation which shed light on some bone modifications, and a morphological description of the carcass had not previously been provided. Here we present the available field data and first full description and analysis of the sediments of the site and this unique specimen, focusing on geology, taphonomy, morphology, genetics, and the carcass condition and handling in the field and laboratory.

2. Material and methods

2.1. Field work

The carcass named the Zhenya Mammoth (also referenced as "Sopochnaya Karga Mammoth"; Gusev et al., 2015) was found on August 28, 2012 (Maschenko et al., 2014a, b; 2015) in the terrace slope of Sopochnaya Karga Cape, Yenisei River mouth, western Taimyr (Fig. 2). At the time of discovery, only the hind limbs and part of the pelvis were visible. The hind feet and tibiae were detached from the carcass and scattered down the slope (https://www.youtube.com/watch?v=WIuwWoAW8C8&feature=youtu.be).

The salvage excavation of the mammoth was headed by Dr. A. Tikhonov and lasted about a week in early September, in daytime temperatures between 0 and +4C, with snow showers occurring during the last days of the field work. Near the carcass, the field crew set up a barrel with water heated by fire that supplied steam to a gun directed at the slope for thawing the frozen sediments (Supplementary Fig. S1, A). The excavation tools included spades, trench shovels, pick-hoes, axes, along with the "zastup" (an axe welded to a long metal pipe for breaking ice for fishing) and "pashnya" (metal pike on a long metal shaft) (Supplementary Fig. S1, B-E; see also https://www.youtube.com/watch?v=YklnU5mF1iA). Before removal, the carcass was propped up by logs (Supplementary Fig. S1, C), and most of the sediments that filled the body cavity were scooped out by a trench shovel (Supplementary Fig. S1, A-C). To get better access to the corpse and facilitate its excavation and removal, the cranium was separated from the carcass, to which it had been loosely attached. The cranial bones had large multiple cracks, with one of them across the tusk alveoli's base, making it possible to transport the detached alveoli bones with tusk separately from the carcass. The rotted soft tissues in the right alveoli allowed the tusk extraction. On the last day of the excavation, the rest of the articulated carcass was dragged down the slope by ropes tied to it (https://www.youtube.com/watch?v=wSaxC3GtekU). The cranium with the attached right hemimandible was rolled down the slope. On the river beach, the excavated mummy's torso, cranium, mandible, as well as the distal hind limbs collected from the slope scree, were loaded onto a sled and pulled to the Sopochnaya Karga helicopter landing site. Unloaded from the sled, the cranium was tied with ropes and dragged on the ground to be

Fig. 1. The mounted skeleton of the Zhenya Mammoth (photo courtesy of Yu. Starikov).

loaded on a helicopter (Supplementary Fig. S1, F). From there, in an unheated cargo plane the still frozen carcass was immediately transported to Dudinka, for temporary storage. On April 17, 2013 the mammoth mummy was delivered to St. Petersburg, and placed in the Zoological Institute freezer for further studies, preservation, and mounting. Before disarticulation of the carcass, about 25–30 buckets of sand that remained in the body cavity were scooped out by metal shovel and rigid scoop; the skin and soft tissues were removed from the bones by metal knives and a scalpel (Yu. Starikov, pers. comm., March 19th, 2016 and January 18th, 2017) (Supplementary Fig. S1, G).

The rescue excavations of the mammoth were performed in cold weather and in a limited time due to restricted availability of the helicopter. Relatively brief daylight, the shortage of human resources, and the lack of lifting machinery limited the data collection and documentation in the field, allowing the recording of only a very approximate position of the carcass in the bank and measurements of its dimensions (*in situ* body length and height in hips; Maschenko et al., 2014a, b; 2015; Pitulko et al., 2016; Suppl.). Mapping the skeleton's position *in situ* and the daily field and photo documentation of the step-by-step mammoth excavation were not performed.

2.2. Lab work. The Mummy's condition, preservation, and studies

The studies of the carcass and bones took place in Zoological Institute (ZIN), St. Petersburg, Russia, in May 2013, followed by the immediate skinning and disarticulation of the skeleton for mounting and soft tissues preservation. The studies of isolated bones were carried out in August–September 2015. At that time, the foot bones were covered by thick layer of soft tissues and were unavailable for this study. All but a small sample (stored in ZIN) of the fine sand removed from the carcass was discarded.

Some of the Zhenya Mammoth bones, especially thin and relatively long bones such as the stylohyoids (inferior rami), ribs, and spinous processes of vertebrae appeared to have shape deformations (Supplementary Fig. S2 and S3 and also see sections 3.3.3.2 and 3.4). During the carcass storage, the bones started drying amplifying these modifications, which had already been visible before the carcass skinning, preparation, and disarticulation. The thinnest bones were more affected, losing their original shapes and acquiring randomly twisted and curved forms. While the carcass drying somewhat contributed to the bones' deformations causing shrinkage, the number of distorted bones was much higher than in any other woolly mammoth skeleton from permafrost that we observed before. The unusual shapes of the bones were noticeable at the time of the excavations and were likely caused by postmortem bone demineralization similar to the process that affected the baby mammoth Lyuba (Fisher et al., 2012).

The samples for AMS dating, histology, and DNA analyses were collected in 2012 and 2014 before the carcass was treated with chemicals for preservation. The treatment began in 2015 and the skinned hide of the torso detached from the legs was preserved separately from the rest of the carcass using standard (modern) tanning methods following Zaslavskiy (1971) with some modifications (Starikov and Petrova, 2016). The legs with the muscles, connective tissues, and skin, and the internal organs and fragments of flesh were soaked in ethanol and dried. The fallen off epiphyses of the limb bones (Supplementary Fig. S4) were glued back together for skeletal mount. The skeleton was mounted in January 2016 and included bones on the right forelimb and feet that had preserved soft tissues. The tanned hide was mounted on the sculpted foam as a representation of the Zhenya's body as it was found *in situ* in the field, to supplement the Zhenya's skeleton exhibit. Both mounts were transported to the Taimyr Regional Museum in Dudinka, for permanent exhibit (http://www.zin.ru/museum/exhibitions/mammoth_zhenya_presentation.html).

Additional fieldwork to collect data for geological description of the Zhenya Mammoth site was performed in July 2014. The icy slopes of the western Taimyr Peninsula reportedly recede about 3–7 m per year (Streletskaya et al., 2009), but the local participant of the Zhenya Mammoth excavation team, Mr. A. Bystrov (Sopkarga Meteorological Station) verified the site's original position from the receded slope, which was gone, leaving no traces of the 2012 excavations. The few days of the fieldwork included preparation, documentation, and description of a geological transect (#1019) close to the former site, along with collection of samples from sediments and the ice wedge for mineralogical, granulometric, and isotopic analyses.

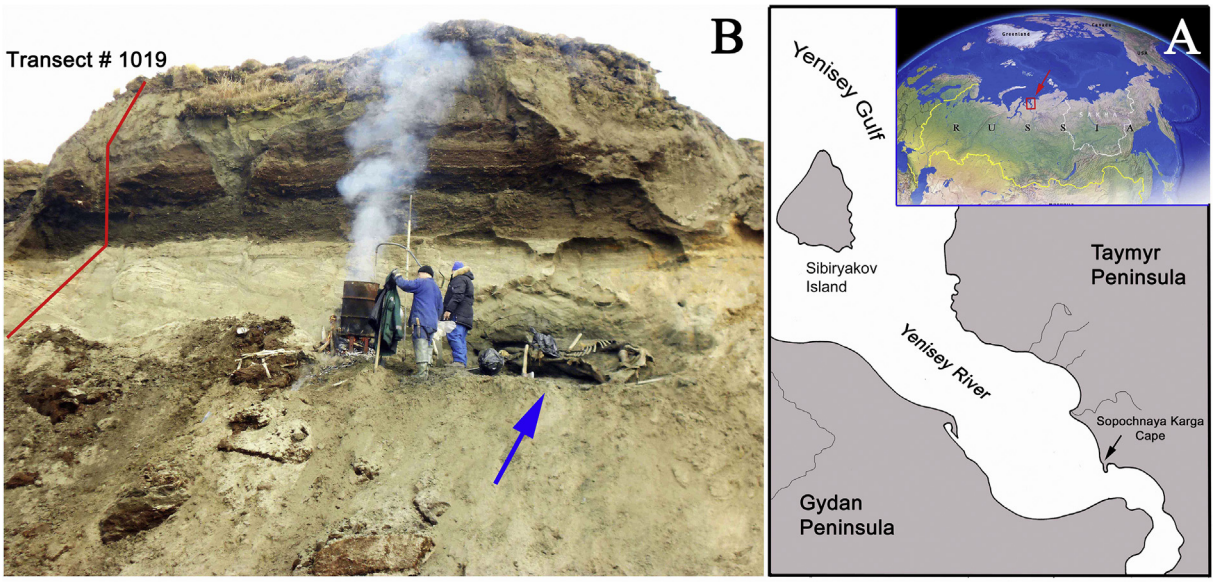

Fig. 2. The Zhenya Mammoth Site. A - geographical locality; B - The Yenisei River terrace slope with the excavated mammoth carcass *in situ* (blue arrow). The red line shows the geological transect #1019 (2014). (For interpretation of the references to colour in this figure legend, the reader is referred to the web version of this article.)

2.3. Material

Most of the bones of the Zhenya Mammoth skeleton were recovered. These include: the cranium; the mandible; the right tusk; a pair of stylohyoids, the basihyoid and thyrohyoid; 43 vertebrae (7 cervical, 21 thoracic, 3 lumbar; 4 sacral, 8 caudal); 21 right ribs and 21 left ribs; the complete sternum; 2 scapulae; 2 humeri; 2 ulnae and radii; the pelvis (2 innominates); 2 femora; 2 tibiae; a left fibular diaphysis and right distal fibular epiphysis; and 2 patellae. All foot bones except the distal phalanges of the right hind foot were preserved covered by soft tissues and skin.

The only bones missing from the skeleton include the left thyrohyoid, parts of both fibulae, three caudal vertebrae (#10–12), the second phalanx of second toe of the right forefoot, and all third phalanges on the hind feet. All the keratinous toe nails and thick sole calluses (about 15–20 mm thick) were detached and gone.

The soft tissues were mostly preserved on the right side, which was in contact with the frozen ground. The hide covered most of the torso and the right ear, forelimbs, and distal hind limbs, and the internal organs (including the penis and remnants of the heart and liver) were preserved. This skeleton was compared with the Yuribei Mammoth (Dubrovo, 1982) and the Yuka Mammoth (Maschenko et al., 2012). The data on the Yuka Mammoth dentition is used as an additional, not published material for this paper.

2.4. Methods

2.4.1. Morphological nomenclature and abbreviations

The bone nomenclature follows Zalenskii (1903), Garutt (1954) and Eales (1926). The measurements were taken by Anthropometer (GPM 101; Switzerland)) and followed the diagrams of Garutt (1954) and Maschenko (2002). Measurements of the upper teeth (denoted using upper case text) and lower teeth (denoted using lower case text) and plate counts follow Garutt and Foronova (1976), which differs from Maglio (1973). The hyoids were measured as shown by Mol and Ligtermoet (1985). Abbreviations used for ribs are R (R1–R21), and for vertebrae C – cervical (C3-C7), T – thoracic (T1–T21), L – lumbar (L1-L4), S – sacral (S1-S4), Ca – caudal (Ca 1-Ca 10/12), Elements or teeth from the right side of the body are designated dex, and from the left side are sin.

2.4.2. Histological analyses

A portion of the heart muscle fragment (atrium, side unidentified) was selected for histological examination. The heart tissue was stored at −18 °C and fixed in neutral 10% formalin at a temperature of 40 °C. The material was subjected to standard histological procedures for the preparation of paraffin sections.

2.4.3. Ancient DNA extraction and sequencing

Following standard protocols for working with ancient DNA (Shapiro and Hofreiter, 2012), before chemical treatment we extracted DNA from two Zhenya Mammoth samples, one cranial fragment and muscle tissue from the vertebrae. We performed all extraction and pre-amplification steps in a dedicated sterile facility at the University of California Santa Cruz Paleogenomics Lab. Briefly, we extracted DNA following Dabney et al. (2013), with modifications suggested by Campos and Gilbert (2012) and Boessenkool et al. (2016). We then prepared Illumina DNA sequencing libraries following Meyer and Kircher (2010), and using Sera-Mag SPRI SpeedBeads (ThermoScientific) in 18% PEG-8000 between each step for library clean up. To enrich libraries for mammoth mitochondrial DNA, we used MYbaits custom bait set (MYcroarray, Ann Arbor, MI) for in-solution hybridization capture of the complete mammoth mitochondrial genome, following the MYcroarray enrichment protocol version 3.01. After incubation, we separated DNA from the probes and purified the enriched libraries with SPRI beads as above. We then made two pools of pre- and post-capture libraries and sequenced each pool on two Illumina MiSeq runs (v3, 2 × 75bp) using 3% and 6% of each run accordingly. We then processed the resulting sequencing data by removing adapters and merging reads with a minimum overlap of 15 base-pairs using SeqPrep (http://github.com/jstjohn/SeqPrep). After verifying the presence of ancient DNA damage at the end of the reads using mapdamage (Jónsson et al., 2013; Supplementary Fig. S8); we mapped the merged reads to previously published *M. primigenius* nuclear (ENA: ERP008929) and mitochondrial (GenBank: NC007596) genomes (Palkopoulou et al., 2015) using bwa (Li and Durbin, 2009). We then assembled the mitochondrial genome using mia (http://github.com/udo-stenzel/mapping-iterativeassembler), calling bases with at least 3X coverage and >75% consensus, so as to avoid false nucleotide calls due to ancient DNA damage.

2.4.4. Phylogenetic reconstruction

We aligned the assembled mitochondrial genome of Zhenya against 102 mammoth mitogenomes published elsewhere (Palkopoulou et al., 2015; Enk et al., 2016), using MUSCLE (Edgar, 2004). We partitioned sequences into four sets: protein-coding genes, tRNA, rRNA genes and D-loop. We specified separate HKY substitution models for each partition, following recommendations of jModelTest2 (Darriba et al., 2012). We then inferred a genealogy of all 103 mammoth mitochondrial genomes using a Bayesian and Maximum Likelihood approach. For the former, we ran MrBayes (Ronquist and Huelsenbeck, 2003) twice, using four MCMC chains and 5 million generations per run and sampling model parameters and trees every 1000 generations. We analyzed parameters for convergence and discarded the first 20% of generations from each run as burn-in. For Maximum Likelihood reconstruction, we used the GTRGAMMA model and rapid bootstrapping algorithm as implemented in RAxML (Stamatakis, 2014). We visualized the resulting phylogenies in Figtree v1.4.2 (http://tree.bio.ed.ac.uk/software/figtree/).

2.4.5. AMS dating

The radiocarbon analysis of the Zhenya Mammoth tibia fragment was performed in the Center for Isotope Research, University of Gröningen, Netherlands.

Standard procedures for the chemical pretreatment of samples followed Mook and Streurman (1983). The collagen was extracted following a procedure originally developed by Longin (1971). The bone mineral was dissolved by repeated treatment with a non-buffered acid solution (1–2% HCl). This took several days, and 10–20% of the bone collagen was dissolved during the process. The crude collagen containing the contaminating carbonaceous substances was washed thoroughly with demineralized water before being treated with slightly acidic (HCl) deionized water. During this treatment, 'pure' collagen dissolved into gelatin, insoluble material was removed by centrifugation, and the gelatin was collected following evaporation. An additional last step was an extra alkali bath for further purification.

The prepared and purified collagen was combusted into gas (CO_2 and N_2) using an Elemental Analyzer, coupled to an Isotope Ratio Mass Spectrometer (IsoCube/IsoPrime). The IRMS provided the stable isotope ratios $^{13}C/^{12}C$, $^{15}N/^{14}N$ as well as the C and N yields.

For ^{14}C analysis, part of the CO_2 was routed to a cryogenic trap to collect the samples for further processing. The CO_2 was transferred into graphite powder by the reaction $CO_2 + 2H_2 \rightarrow 2H_2O + C$ at a temperature of 600 °C and using Fe powder as a catalyst (Aerts et al., 2001).

Next, the graphite was pressed into target holders for the ion

source of the AMS. The AMS then measured the $^{14}C/^{12}C$ and $^{13}C/^{12}C$ ratios of the graphite (van der Plicht et al., 2000). From these numbers, the conventional ^{14}C age was calculated and calibrated into calendar ages using the calibration curve IntCal13 (Reimer et al., 2013). The calibrated ages are reported in calBP, which are calendar ages relative to 1950 AD. The stable isotope ratios are defined as the deviation of the rare to abundant isotope ratio from that of a reference material, expressed in permil and using the reference materials VPDB for $\delta^{13}C$ and ambient air for $\delta^{15}N$ (Mook, 2006)

2.4.6. Sediment analyses

The collected samples (n = 23) were used for granulometric analyses, salinity, organic carbon content and others, adding to over 200 Sopochnaya Karga database specimens. The dates' calibrations (CalPal) cited in Section 3.1 were performed at the University of Cologne in 2008 by U. Danzeglocke, W. Weninger, O. Jris (www.calpal.de). Granulometric analysis was performed following standard procedures (GOST 12536-2014 (Earth); GOST 26423-85, GOST 26424-85, GOST 26425-85, GOST 26426-85 and GOST 26428-85 (Soils); GOST 23740-79 (Earth).

3. Results

3.1. Geology

3.1.1. The Sopochnaya Karga (SK) coastal exposure

The coastal exposures of lower parts of the Yenisei River are considered to be characteristic of Pleistocene – Holocene sedimentation conditions for this part of the Arctic, which were largely influenced by the transgressive and regressive stages of the Arctic Sea basin. The marine transgressions generally caused a degradation of continental permafrost, while regressions resulted in aggradation of permafrost on the exposed Arctic sea shelves.

Paleostratigraphic study of the northern Yenisei River region suggests that marine transgression and corresponding marine sedimentation occurred 145-70 kyrs BP (= MIS 6 and MIS 5) comprising three thermal maxima alternating with episodes of colder periods at around 130, 115, 100 and 75 kyrs BP (Molodkov and Bolikhovskaya, 2009). Marine sedimentation was replaced in this area by continental deposits about 70 kyrs BP. During the Zyryanka glaciation (71–11.7 kyrs BP; MIS 4-2) the overall climate in Western Siberia was cold and dry (Astakhov, 2013).

Alternation of warm and cold climate phases resulted in complex composition of various sediment types characteristic for northern parts of the Yenisei River, including the study area located near Sopochnaya Karga Cape. Here, the 2 km long coastal exposure represents frozen Quaternary deposits exposed in 12–20 m high terrace. The exposed sediments are comprised of horizons of continental and marine sediments (Streletskaya et al., 2006, 2007, 2009, 2013a, b; Gusev et al., 2011), which were correlated with the Zhenya Mammoth site section #1019.

3.1.2. The Zhenya Mammoth site

The site coordinates are 71°45′09.2″ N, 82°40′19.6″E. It is located on the east bank of the Yenisei River Gulf about 3 km north from the polar meteorological station "Sopochnaya Karga" on Sopochnaya Karga Cape on the western Taimyr Peninsula.

The thickness of the exposed bank sediments in this location (#1019) is 12 m (Fig. 3). The top of the permafrost is 0.9 m below the surface, below which all sediments are frozen.

Unit I (0–4.5 m from the surface) consists of alternating layers of sandy loams and peat (Fig. 3 A, Supplementary Fig. 5; Supplementary Table S1). The upper layer is partially decomposed peat that is present in most of studied coastal transections of Sopochnaya Karga Cape and has a depth of 1–2 m (Figs. 3 and 4). A woody material found at the base of the peat horizon is dated as 10,210 ± 70 cal BP (C^{14} 9050 B.P.; DR-6545), and the peat age is 11,460 ± 400 cal BP (C^{14} 9900 ± 230 B.P.; DR-6543).

The "peat layer" overlies the silty and sandy-loam of brown color and includes unevenly distributed remains of peat and small plant roots. The thickness of the peat interlayers varies from 2-5 cm to 20–25 cm. The peat is slightly decomposed. The upper part of the frozen section, from 0.9 to 1.4 m depth, is characterized by micro-layered cryostructure with a total moisture content of up to 66%.

Unit II (4.5–7.4 m) is largely composed of medium to fine-grained gray and yellow sands. In SK coastal transects, this unit may be 10 m thick (Fig. 3, Supplementary Fig. S5). The Unit's upper portion (4.7 m) contains a ~10 cm thick horizon of pebbles mixed with sand. The pebble sizes vary from 0.1 to 1.2 cm in diameter with a predominance of smaller fractions. The pebble horizon is underlain by horizontal and cross-bedded sands with a dip of 30–45°. The sand horizon is characterized by a relatively homogeneous distribution of plant remains including small branches of shrubs, and in corresponding SK deposits it contains ferruginous spots and has organic carbon content up to 2.0%. The unit is frozen and has a massive cryostructure with rare single ice lenses that do not exceed 1 mm in thickness. Moisture (ice content) of the sand is uniform (22–25%) along the profile.

The mammoth carcass was found in this unit at 6 m depth from the surface (Fig. 4 A) with the torso filled with fine gray sand with occasional plant remains. It's head was facing the ice wedge north of the carcass (Maschenko et al., 2015). The sands surrounding the embedded carcass and the overlying sands are homogeneous through this unit with no apparent changes in sedimentation or apparent boundaries indicative of substituted facies. The radiocarbon dates obtained from the deposit sequences correspond to the general scheme of constrative (Lomakin, 1948) sediment accumulation.

The mineralogical components and the graulometric characteristics of the sediments composed of fine sands and loams of this Unit show a similar pattern with the corresponding units of other SK transects (Streletskaya et al., 2005, 2007, 2008, 2009, 2011; Romanenko et al., 2005; Gusev et al., 2011) and indicate that the accumulation of this Unit was not created by fast water currents or occurred in the river channel as reported earlier (Gusev et al., 2015; Pitulko et al., 2016). The layered sandy loams and sands in the upper part of the unit that included the mammoth carcass represent syngenetically deposited alluvial-lacustrine sediments of a wide floodplain, which were periodically inundated by flood waters. This pattern of alluvial-lacustrine accumulation of deposits simultaneously followed by freezing is confirmed by persistently high ice content of sediments and presence of syngenetic ice wedges in the section. The deposition of the sands of this unit occurred during an early phase of MIS 3 when the Yenisei Gulf was inundated by a transgression of the Kara Sea; however, the site was never covered by marine transgression (Streletskaya et al., 2009; 2013a,b; Oblogov, 2015).

The pattern of the accumulation of the deposits as characterized above excludes the possibility of movement of any object during the Unit formation. Moreover, it is known that complete corpses retaining the anatomically articulated body of large and heavy animals usually indicate minimum movement before burial, or the lack of transportation (Efremov, 1950), and the Zhenya Mammoth fits this scenario. The combined evidence indicates the *in situ* burial and preservation of the mammoth carcass.

Unit III (7.4–9.1 m) is topped by a 20 cm thick pebble layer. The pebbles are 1 mm–7 cm in diameter with varying degrees of roundness, and are underlain by yellow-gray and dark-gray sandy

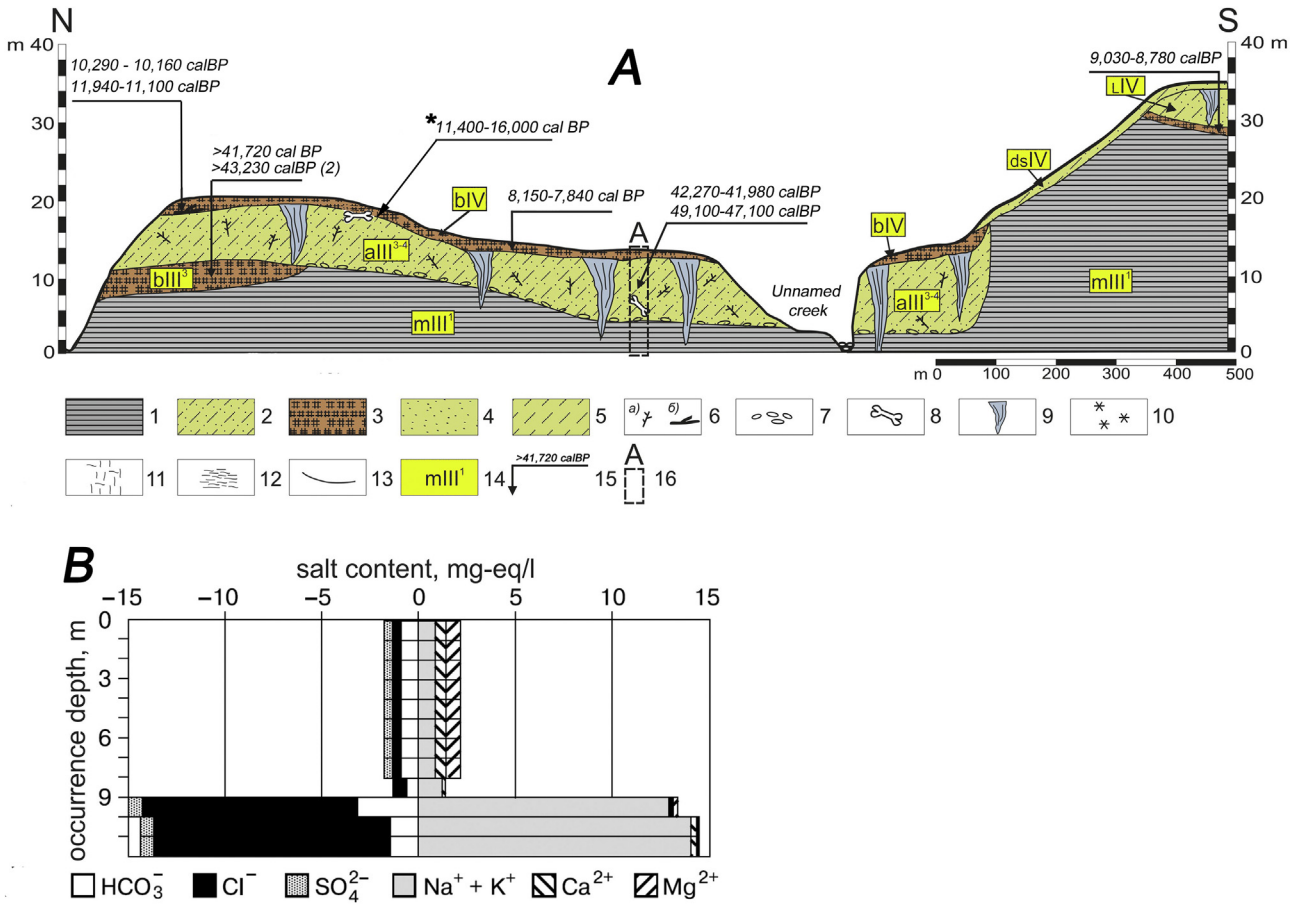

Fig. 3. The combined geological coastal section of the Yenisei River terrace with the Zhenya Mammoth locality on Sopochnaya Karga Cape (A) and the ion content distribution of water-soluble salts in the sediments (B) (Streletskaya et al., 2007). 1 – clay; 2 – sandy loam and sands; 3 – peat; 4 – sands; 5 – sandy loam; 6 – plant inclusions (a – twigs, b – tree trunks and stumps fragments, about 5–6 mm in diameter); 7 – pebble inclusions; 8 – mammal bones; 9 – syngenetic ice wedges (shown not to scale); 10–12 cryogenic textures: 10 – massive; 11 – incompletely reticulate; 12 – micro-layered; 13 – sediment boundaries; 14 – sediment types and ages; 15 – sediment geological dates; 16 – the Zhenya Mammoth Site section (this study). Abbreviations: alll (3–4) - alluvial deposits (MIS 3-MIS2); mll1 (1) – marine deposits (MIS 5); blll (3) – biogenic (peat) deposits (MIS 3); bIV – biogenic (peat) deposits (Holocene); dslV – the Holoene deluvial and solifluction deposits; LIV - lacustrine deposits (Holocene).* - probable original location of the bones found on the slope scree. The 14C dates from Gusev et al. (2011) and Streletskaya et al. (2013) are calibrated following Reimer et al. (2013).

loam and sand with inclusions of organic particles and rare black pebbles (Fig. 5). The black pebbles are up to 3 cm in diameter and composed of claystones or argillites of Cretaceous or pre- Quaternary age. The coarse grain composition of sandy loam and sand of this unit represents alluvial deposits of the powerful river and are comparable to the modern riverbed deposits about 300 km upstream (Streletskaya et al., 2005; 2007). The unit has massive cryostructures with sporadic multi-directional ice lenses not exceeding 1 mm in thickness.

The sandy loam, peat, and sands in Units I-III and corresponding SK deposits are not saline; the salt content does not exceed 0.06%. Sodium and hydrocarbonate ions are dominant (Fig. 3, B). Within the SK coastal transects the lower boundary of the corresponding deposits (sands and sandy loams) is uneven and lies at elevations from 2 to 12 m above sea level. The northern part of the exposure is underlain by a 3 m lens of peat (depth 8–12 m), which has a calibrated age over 41,720 cal BP. Occurrences of large peat lenses in other SK sections are indicative of widespread coastal marshes under relatively mild climatic conditions.

The sand on the contact with the underlying clays in the SK sections often includes pebbles and small boulders of varying degrees of roundness with a few fragments of shells and remnants of wood inclusions.

Unit IV (horizon below 9.1 m). This thick layer is incompletely reticulate and measures 2.9 m above the sea level, with the lower boundary reaching below the sea level. It is represented by brown-gray and dark clays with streaks and spots of iron, single inclusions of pebbles, and black spots of organic matter with a diameter less than 1 mm (Fig. 3, A, Supplementary Fig. S5). The amount of organic carbon in the clay sediments is 0.8–1.0% (Fig. 4 B). The clays in this and other SK units have marine genesis, as sediments are saline (salinity 0.2–1.0%) and have characteristic sodium chloride composition. The depth of the upper clay boundary in other SK sections varies from 2 to 30 m above ground. The ice lenses below 9.9 m in these transects are oriented predominantly sub-vertically.

Ice Wedges and Climate. The lower part of the ice wedges found in the clay sediments were formed epigenetically soon after the daylight surface was exposed to the atmospheric conditions (Fig. 4 A). The upper part of the ice wedges were formed in conditions of a floodplain regime.

Increase of a silt fraction and the size of the syngenetic ice wedges from the bottom to the top of the site profile are indicative of cold climate during the time of terrestrial sedimentation. Near the contact with the ice wedges the sediments showed an increase in the ice content. The sands and sandy loams (0.7–4.5 m depth) are identified as syncryogenic floodplain facies of alluvium, which is inferred from cryogenic structure and presence of roots *in situ*.

Formation of these sediment types in this region in the early

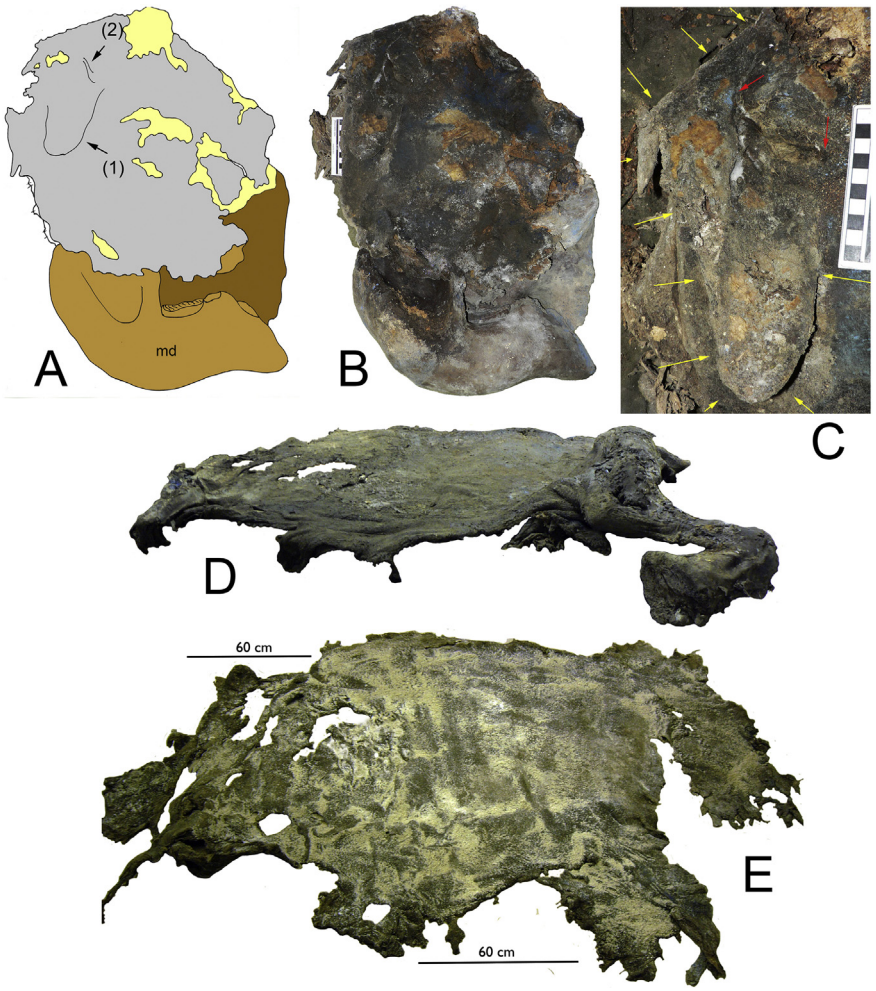

Fig. 4. The Zhenya Mammoth head and the hide. A, B – the right side of the head before preparation; A – locations of the preserved skin: gray – remnants of the skin, yellow – heavily deteriorated epidermis, brown - bone, dark brown – frozen sediment; md – right hemimandible; (1) - ear lobe, (2) – auditory meatus; C- right ear, yellow arrows - auricle contour, red arrows – the dorsal and ventral corners of the auditory meatus; D – the hide with attached right foreleg where it was preserved on the elbow and forefoot; E – the removed hide from the carcass (photo courtesy of Yu. Starikov). Scale 1 cm where not labeled. (For interpretation of the references to colour in this figure legend, the reader is referred to the web version of this article.)

Zyryanka time (MIS 4) was determined by climatic cooling and regression of the Arctic sea, when marine sedimentation was replaced by continental pattern of deposit accumulation. Subsequently, exposed land surfaces and islands where continental deposits were accumulated became syngenetically frozen, along with formation of the large syngenetic ice wedges. Average winter temperatures reconstructed from isotopic composition of ice wedges during MIS3 were −23 °C - −25 °C. This is 5–7 °C higher than currently in the coastal Western Siberia, and 6–8 °C higher than in the Taimyr Peninsula (Streletskaya et al., 2009, 2014).

3.2. Geological age

The processed sample (tibia) of the Zhenya Mammoth showed excellent preservation of the collagen, with the C and N parameters and stable isotope ratios $\delta^{13}C$ and $\delta^{15}N$ well within their expected ranges in the table shown below and Supplementary Fig. S6.

The oldest ^{14}C age of Zhenya (44,750 BP) is not too far from the limit of the ^{14}C method (van der Plicht and Palstra, 2016). In this case, the measured ^{14}C activity of the sample is well above the anthracite blanks (by about a factor of 2). This fact and the excellent quality of the bone suggests that the date of Zhenya is reliable.

Other dates for Zhenya (Supplementary Table S2) were determined by the University of Georgia, Athens, USA (laboratory number UGAMS; Maschenko et al., 2014a, b), soon after the discovery of the mammoth. The samples received the same pretreatment as was applied in Gröningen. A small sample of bone yielded a date of 37,830 ± 160 BP (UGAMS-12565), much younger than the Groningen date. The bone was a fragment of the left ilium, which is porous and therefore methodologically problematic; contamination with allochthonous carbon cannot be excluded. Moreover, the C and N quality parameters of this sample were not available (Cherkinsky, personal communication).

Laboratory N	^{14}C age BP	$\delta^{13}C$ (‰) (VPDB)	C%	$\delta^{15}N$ (‰ (Ambient air)	N%	C/N	Calibrated age (calBP)
GrA-57723	44,750 (+950/-700)	−22.09	48.3	6.84	17.5	3/2	49,150-47,100 (± 1 σ)

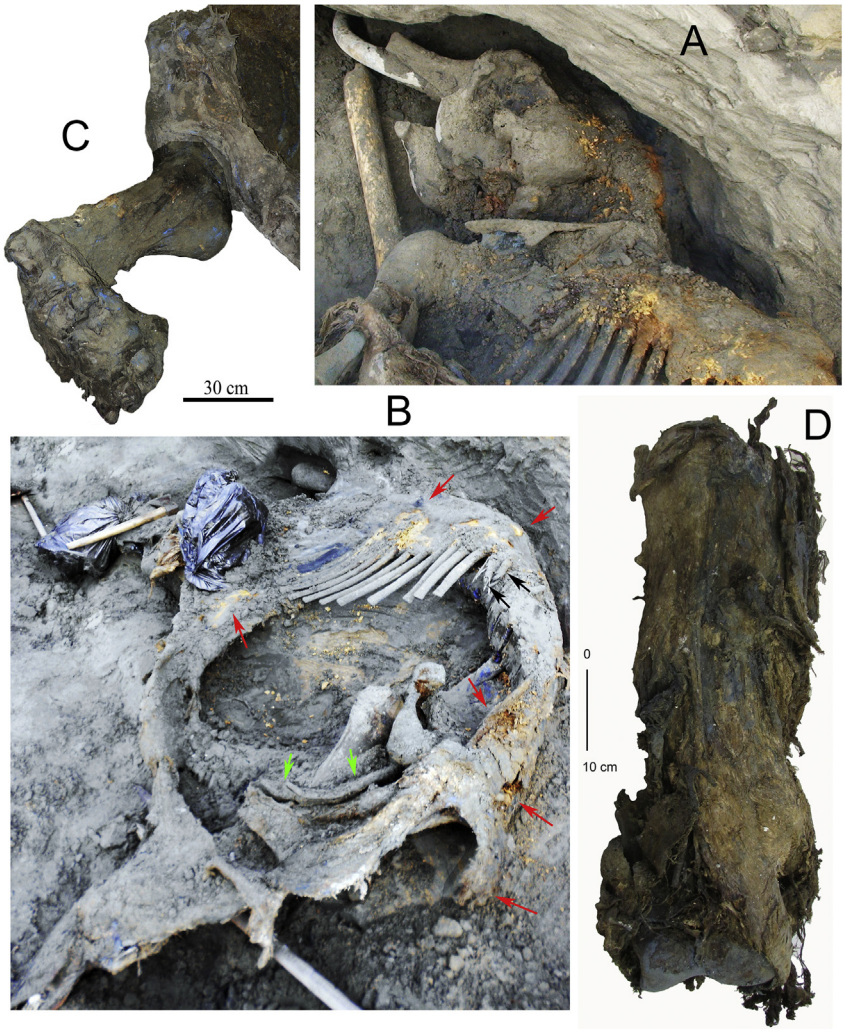

Fig. 5. The Zhenya Mammoth carcass *in situ* and the right forelimb. A – the head and frontal torso of the carcass *in situ* (notice especially thick yellow fat deposits in the nuchal, neck, and upper torso areas, and blue vivianite powder on the scapula and ribs); B – the back of the torso *in situ* (red arrows show the extensive fat deposits; green – the penis, black – last two ribs broken off during excavations); C – the right forelimb with manus connected to the torso (notice dry ligaments and vivianite covering the surfaces), D – the right humerus covered by soft tissues, cranial view. (For interpretation of the references to colour in this figure legend, the reader is referred to the web version of this article.)

The same laboratory also dated hair and muscle tissue from Zhenya. The hair sample dated 41,100 ± 190 BP (UGAMS-12567), also significantly younger than the Gröningen date. It is known that for samples this old, hair often dates younger than bone collagen, as was the case for the baby mammoth Lyuba (see Kosintsev et al., 2012). Such samples are more subject to contamination with foreign carbon. The muscle tissue dated 43,350 ± 240 BP (UGAMS-12566), a bit younger than the Gröningen bone date, but these two dates are consistent at the 2-sigma confidence level. Commonly, the oldest date should be considered the most accurate one, because contamination is more often caused by younger rather than older carbon.

Based on these direct dates, we conclude that Zhenya must have died about 48,000 (calendar) years ago. Pitulko et al. (2016) stated the age as being 45,000 years old, but the latter refers to ^{14}C years (in BP), and not calendar years. Pitulko et al. (2016) also showed additional dates from the deposits in which Zhenya was discovered. Large samples of the organic matter from the deposits were dated by the conventional ^{14}C method (liquid scintillation counting) in St. Petersburg, Russia. In stratigraphic order, the dates are: 18,200 (+2600,-2200) BP (LE-9823), 36,000 ± 2500 BP (LE-9822) and 47,600 (+10,200/-4400) BP (LE-9821). The first two dates represent the top and bottom of a peat layer; the 3rd is a willow branch fragment found in the floodplain deposit (see Pitulko et al., 2016, Fig. 1D). These dated materials from the deposits were above the mammoth, which dated about 45,000 BP. It seems that the willow branch date is a bit off; however, the 1-sigma range of the date as published is 43,200-57,800 BP. The latter number is not reliable and in our view the date of LE-9821 should be considered as "older than 43,000".

Given this, the stratigraphy of the three deposit dates and the date for the mammoth are consistent. This applies to the selected bone date (GrA-57723) as well as to the muscle tissue date (UGAMS-12566).

3.3. Carcass description

3.3.1. Soft tissue exterior morphology

3.3.1.1. Head. The soft tissues covering the mandible were gone as well as those from the left side of the cranium. However, very deteriorated skin was preserved on the cranium's right side (Fig. 4, A and B). The preserved right ear had a short (2 cm long, 0.5 cm wide) ear opening in a shape of sub-vertical groove (Fig. 4, C). The height of the preserved fragment of the ear between the tip of the

lobe to the upper edge of the fragment slightly above the end of the ear opening groove measured 25 cm, and its full height is estimated at about 30 cm. The lobe was 9.5 cm high and 8.5 cm wide at the base. Based on the sizes of the ears of the Adams, Khatanga, and Yukagir Mammoths (between 30.7 cm and 38 cm high; Vereschagin and Tikhonov, 1999, Mol et al., 2006), the estimated total width of the Zhenya Mammoth's ear was about 17 cm. Short and coarse hair about 5–15 mm long was preserved around the ear opening.

The cranial cavity contained fragments of brain tissues in the form of lumps of yellow and brown matrix with preserved pieces of *dura mater*, a brain tissue often preserved better than other brain tissues in other mammoth specimens, as reported for baby Dima (Vereschagin, 1981), baby Masha (Vereschagin, 1999) and Yuka (Kharlamova et al., 2016).

3.3.1.2. Hide. The skin, mummified muscles and tendons, and fat were mostly preserved on the right side of the body, but had signs of decomposition. These tissues were present on the entirety of the front legs, feet, and some on the distal tibiae. The skinned and preserved hide on the right side of the body measured about 2.5 square meters (24,660 sq. cm) and although the Zhenya individual was not an adult, the size of the single fragment of hide is among the largest known all woolly mammoth specimens (Fig. 4, D and E). Its size was comparable to the hide of the Berezovka Mammoth (skin from left and right sides of the body and belly; Herz, 1902) and the Yuka Mammoth (an almost complete hide from a juvenile; Boeskorov et al., 2014) and exceeded the hide sizes that were reported for the Eterikan Mammoth from Bolshoi Lyakhovsky Island (200 × 120 cm; Lazarev, 2002), Sanga-Yuruyakh Mammoth (149 × 117 cm; Vereschagin and Tikhonov, 1999), Kieng-Yuaryakh Mammoth basin (200 × 100 cm; Lazarev, 1980) from Eastern Siberia and Yuribei Mammoth (20 × 30 cm; Sokolov and Sumina, 1982) from Taimyr Peninsula. The Zhenya Mammoth hide had scarce, short, rare hairs frozen to the right half of the body, and lacked any trace of vivianite. Conversely, the exposed muscle tissues and bones of the skyward left side of the body were littered by spots of fine-grained vivianite. Moreover, similar to the “second category” of vivianite determined for the baby Lyuba (Fisher et al., 2014), this mineral was detected on the bones under the soft tissues of the right side of the Zhenya Mammoth's body. The spatial distribution of the vivianite indicates differences in micro-environments and microbial activities (McGowan and Prangnell, 2006; Rothe et al., 2016) that took place within the Zhenya Mammoth body.

3.3.1.3. Fat. Dull-yellow adipocere deposits continuously covered the entire neck area (up to 5 cm thick), the dorsal surface of the longitudinal muscle fascia on the back, and the sacral parts (Fig. 5, A-C). At the first thoracic vertebra the dorsal fat deposits were over 15 cm thick, which decreased gradually towards the sacral part, forming a 3–4 cm thick layer. Deposits of subcutaneous fat reaching 9 cm thickness were also reported for the Berezovka Mammoth (Hertz, 1902). Deposits of the 7 cm thick fat in the neck area were also found in the Oimyakon baby, which continued onto the body side, forming a ~2 cm thick layer (Boeskorov et al., 2007). The baby Lyuba Mammoth also had similar fat deposits in the neck area, which were identified as a brown fat (Fisher et al., 2012), the tissue involved in thermogenesis.

3.3.1.4. Limbs. Among the upper limbs only the right humerus preserved most of the mummified soft tissues; however, the skin was missing on all but the caudal side above the elbow (Figs. 4, D and 5, D). The feet, covered by muscles and tendons in different degrees, were preserved from the soles to the wrists and ankles (Figs. 1 and 5C and D; also see 3.3.3.8). The skin, muscles, and the thick coarse base of the sole were missing on the left forefoot, together with a few distal phalanges. The sole skin on the right forefoot and both hind feet were preserved, but all of these were missing the thick coarse bases. Nail plates were missing on all of the feet and their attachment surfaces on the remaining hide of the soles were not clearly detectable for measurements. The main carcass measurements taken in field and lab are given in the Supplementary Table S3.

In the body cavity, small fragments of the heart and liver were discovered (see section 3.3.2).

3.3.2. Internal organs

3.3.2.1. Gross morphology

3.3.2.1.1. Heart. The preserved atrium fragment (60 × 89 mm) was gray in color and had a distinctive fibrous structure. The wall thickness measured 35 mm in a frozen state.

3.3.2.1.2. Liver. A small piece of the liver tissue with a weight of under 20 g had an even brown color and lacked most of its structure. The whole fragment was completely incorporated into parasitological and histological studies, which yielded the presence of the eggs of nematodes and cestodes, the first record of such kinds of parasites being found in woolly mammoth (Glamazdin et al., 2014a, b).

3.3.2.1.3. Penis. (Fig. 5, B; Fig. 6, A-C). The penis appeared to be the only well-preserved internal organ of the Zhenya Mammoth specimen. This is the fourth penis ever recorded for the species, and was previously reported for the Lyakhovky Mammoth (Vollosovich, 1914), the baby Dima (Vereschagin, 1981), and the Berezovka Mammoth (Hertz, 1902; Zalenskii, 1903) from eastern Siberia.

At the time of the discovery, the penis was positioned in the body *in situ*, cranially from the pelvis, corresponding to the condition of retracted organ. Its caudal part was located above the frontal edge of the pubic bones, but ligaments securing the penis base to the pubic symphysis were lacking. The penis ligaments were located approximately 20 cm below the reconstructed skin fold of the anus, and the main bundle of the ligaments was located about 20 cm below the level of the fusion line of the greater trochanter's epiphysis on the femur. This part of the penis was also covered by ligaments under the circular muscles of the remaining fragment of the very short (about 5–7 cm) rectum. Muscles and longitudinal bundles of connective tissues surrounded and ran along the base of the penis. The thickness of the connective tissue around the penis was about 2–2.5 cm. The base of the penis was bent with its convex surface directed caudally. The opposite curvatures of the base and its distal portion gave the penis an S-shape.

A visible constriction for ligaments marked the boundary of the penis protrusion from the preputial ostium. This protruding portion (free part of the penis) measured about 65–67 cm. The total length of the penis was about 98 cm (Maschenko et al., 2015), exceeding that of the baby Dima (30 cm: Vereschagin, 1981) and the Berezovka Mammoth (from preputial ostium 105/86 cm; Hertz, 1902), and is comparable to those in the Asian elephant (100 cm; Shoshani and Eisenberg, 1982). Unlike the penis morphology of the Berezovka and the baby Dima mammoths (Vereschagin, 1981; Vereschagin and Tikhonov, 1999), the “glans penis” in the Zhenya Mammoth was not distinguishable. However, its distal part was slightly bent ventrally, and this “apex” had an approximate length 22 cm. At the time of the study the penis was found mediolaterally compressed at the distal end with larger dorsoventral diameter (5 cm) than that (4 cm) in the middle part. The dorsoventral diameter at the penis base was 6.5 cm larger than measured at the constriction.

A preserved fragment of urethra (Fig. 6, B and C), represented by a thick-walled tissue of oval shape in cross section, was detected at

the middle part of the penis protruding beyond the prepuce. The urogenital opening was not found. Surrounded by a layer of very dense connective tissue, the urethra extended along the dorsal surface of the penis, where its detectable part was over 20 cm long. The transverse diameter of the urethra with the connective tissue was 1.3–2 cm. Its protrusion through the dorsal surface of the penis was due to the deterioration of soft tissues and its close position to the dorsal surface of the *corpora cavernosa*.

3.3.2.1.4. Histology of internal organs. Stained with hematoxylin -eosin, the eosinophil-dyed tissues lacked traces of residues of nuclear structure (Supplementary Fig. S7, A–D). The heart tissue, when stained with Mallory's Connective Tissue Stain, appeared as unstructured red remnants with the rare inclusions of blue (Supplementary Fig. S7, B). While blue inclusions were not possible to identify, the red-colored filaments were identified as the remains of the muscle tissue (Supplementary Fig. S7, C, D). There were no residues of cell or nuclear structures identified.

3.3.3. Skeleton

3.3.3.1. Cranium and teeth

3.3.3.1.1. Cranium. (Figs. 7 and 8). The upper left and right teeth (Dp4/M1) were symmetrically developed and were in the same stage of wear (Fig. 8, F). The right tusk socket had normal shape (Fig. 8, A), while the absence of the left tusk in the under-developed left maxilla produced asymmetry of the skull (Fig. 7, A). Consequently, the left tuskless premaxillary (*premaxilla*) and the maxillary process (*processus maxillaris*) developed a dorso-ventrally flattened conical shape, filling the undeveloped alveolus with spongy bone (Fig. 7, B, D). The tuskless opening was 24.0 mm wide, 14.5 mm high at the edge, and 93 mm deep. The internal shape of the right alveolus was normal. Other cranial bones do not exhibit unusual morphologies or sizes (Supplementary Table S4). The lower edge of the nasal openings was at the level of the upper third of the orbit. The lower edge of the external ear canal was at the level of the upper edge of the zygomatic bone. The nasal process of the nasal bones barely protruded beyond the level of the frontal bones. The vertical extension of the central occipital depression (*fossae occipitalis*) was almost equal to the height of the occipital squama (Fig. 7, E), significantly exceeding this relative size in juveniles and adults of the modern African elephant. There was a preserved vertical thin external crista subdividing the depression into two parts, and additional small ridges on the bottom.

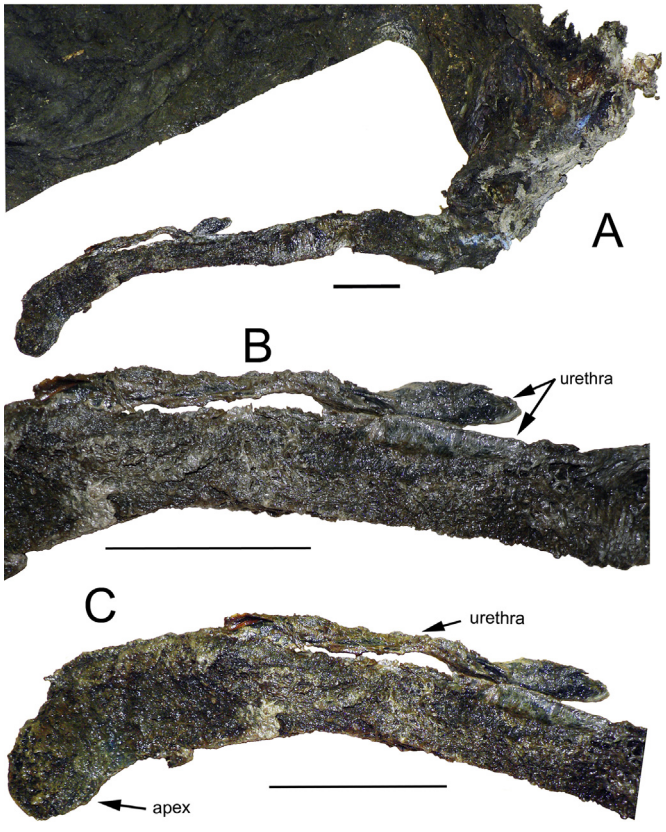

Fig. 6. The Zhenya Mammoth penis. (A) – the penis connected to the body, and (B, C) - extracted from the carcass. Scale 10 cm.

Most of the sutures on the exterior of the cranium were unfused. The dorsal, lateral, and caudal sides of the cranium had unfused sutures between paired bones connected with each other, such as premaxillaries, maxillaries, nasals, and frontals (Fig. 7, A). The maxillary-premaxillary (on lateral surface), nasal and premaxillary (nasal process), frontal and premaxillary (nasal process), maxillary (zygomatic process) and zygomatic, temporal (zygomatic process) and zygomatic, temporal and parietal, and occipital and temporal bones also had unfused sutures (Fig. 7, E, C). When African elephants reach ~6 months of age (age group II; Laws, 1966) the sutures between the maxillary and premaxillary (palatine process) on the ventral side of the cranium are almost entirely obliterated (Van den Merwe et al., 1995); the Zhenya Mammoth bones have a similar condition.

The cranium base that became detached from the rest of the skull showed the absence of fusion with the temporals (squamous part), presphenoid, vomer, and maxillaries (Fig. 7, C). It had a clear and strongly convoluted line between the lateral occipitals and barely detectable fusion boundaries between the following bones: basioccipital and temporals (*bulla tympanica*) (=closed petrooccipital fissura), temporal (musular process of *bulla tympanica*) and basisphenoid and basisphenoid-pterygoid, which can be considered as the fused sutures. The presphenoid remained unfused with basisphenoid. It was not possible to determine the fusion status of the presphenoid with the vomer, and the ethmoid with other bones, as well as the palatines with each other and with maxillaries. Most likely, the fusion between these bones remained uncompleted.

During storage of the carcass bones between fall 2012 and spring 2013, the occipital sutures of the cranium expanded into large gaps, and several joined together basal bones loosened and separated from the skull. The pterigoid processes of the basisphenoid bones that formed the caudal wall of the M2 alveoli also separated and fell off during storage, exposing very thin maxillary edges of the alveoli (Fig. 8, B, J, K). These closed alveoli contained an underdeveloped M2 (Fig. 8, G-I), which appeared to be loose in the closed cavities and was carefully collected for the study.

The cranium had few cracks and damage on its surface. All damage and soft tissue deterioration were mainly located on the left side of the carcass, which during the burial process was directly exposed to the elements, and had possibly remained available to scavengers (damage to the soft tissues only) and had been subjected to weight and abrasion of the overlying deposits. The damage on bone surfaces was moderate, showing signs of the sediments' abrasion and deterioration, degrading the thin cortical wall and exposing highly pneumatized bone. These damaged locations were represented by a large section on the upper left occipital squama, small region on the upper right occipital squama, an area along the nuchal crest, and a strip on the left side from the nuchal crest along the temporal line and the dorsal side of the nasal process of premaxilla. Long exposure to the dry conditions might have caused similar deterioration of the other bones, especially those with a very thin cortex.

There were three large cracks on the cranium. The first crack

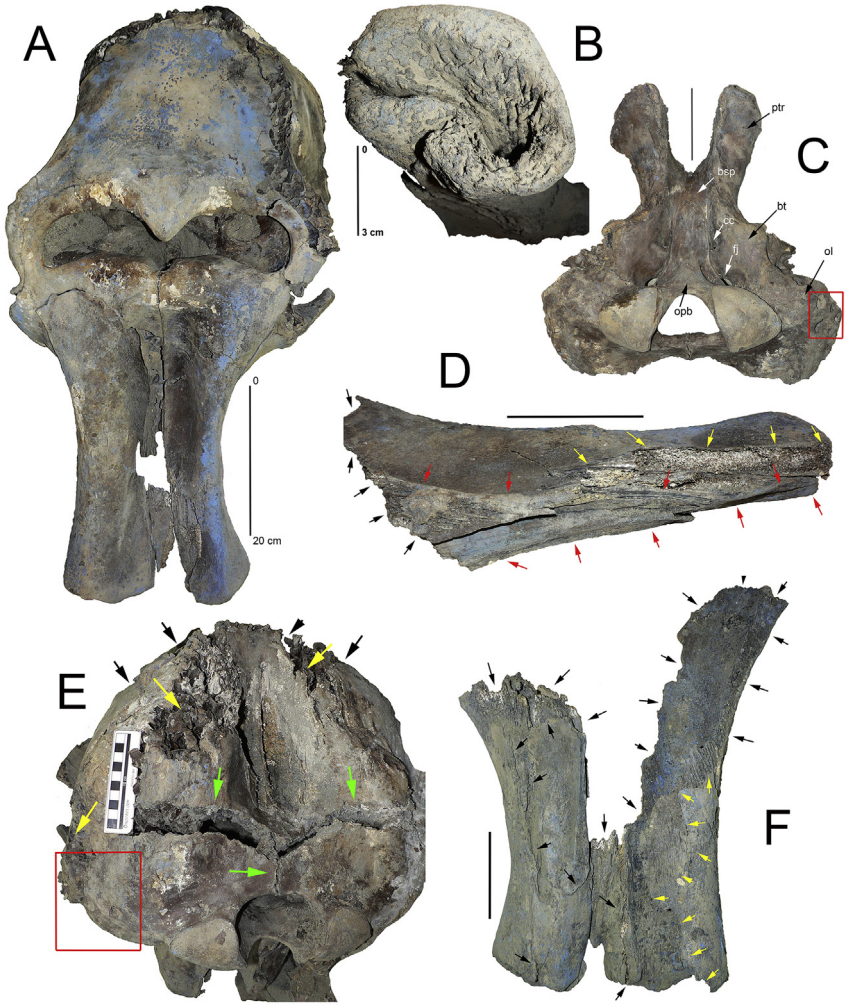

Fig. 7. The Zhenya Mammoth cranium and its bones. **A** – the cranium in assembled position, dorsal view (notice longitudinal cracks along the alveoli and powdered vivianite on the surface); **B** – the left deformed socket of the undeveloped left tusk, ventrocranial view; **C** – the basal part of the cranium (bsp – basispehnoid, bt – tympanic bulla, cc – carotid canal, fj – jugal foramen, ptr – pterygoid, ol – lateral occipital bone, opb – basilar occipital, red square – location of the lesions; **D** – the left deformed alveolus (of the undeveloped tusk), mediocaudal view (arrows: black - transversal "dry" break, yellow – "dry" break on the dorsal side, red – "green" break" on the ventral side); **E** – occipital side of the cranium (arrows; yellow – broken off surface areas ("dry" breaks, natural deterioration), black – broken off cortical bone along the nuchal crest ("dry" breaks, natural deterioration), green – opened gaps along the fusion lines of the occipital bones; red box - location of the bone lesions; **F** – dorsal side of the tusk alveoli (arrows: black - "dry" breaks and natural deteriorations, yellow – edges of the medially flaked off ("dry" breaks, natural deterioration) cortical bone on the left praemaxilla. Scale 10 cm where not labeled. (For interpretation of the references to colour in this figure legend, the reader is referred to the web version of this article.)

went through it transversally leaving a sub-horizontal line just below the nasal opening. The second crack connected to the first followed the fusion line between the maxillary and premaxillary on the right side of the cranium and occurred together with the third large crack. This third crack developed longitudinally between the left and right tusk alveoli following the intermaxillaries' fusion line, as if the bones collapsed from not being able to sustain the vertical pressure of the sediment weight and broke where the bones were the weakest. This ventral side of this longitudinal crack had a "green" break (Fig. 7, D) and occurred in the cranium, which had retained a relatively high content of collagen. These three cracks split the cranium into three major parts, which sediments supported in place, preventing the fragments from falling apart until the carcass was excavated. Further fragmentation of cranial bones continued during the storage in the lab for several months at room temperature. There, the broken off alveolus for the tusk became fragmented further in the proximal part, exhibiting "dry" breaks and signs of deterioration. Neither of these fragments demonstrate marks of dynamic impacts, hackle marks, or prepared striking platforms, which are characteristic of intentional strikes caused by human artifacts; such impacts had been previously claimed, and the damaged portion of the skull was termed the "desired direction of impact" (Pitulko et al., 2016, Fig. 3A).

On the lateroventral side of the left latero-occipital bone, there were six shallow (about 5 mm deep) round and oval lesions detected (Fig. 7, C, E; Fig. 8, C). The sizes of these holes varied between 0.7 × 0.9 cm to 1.5 × 1.6 cm. The lesions had well defined edges on the cortical bone (surface), and porous and deteriorated bone structure sides on the sides and bottoms of the holes. Lesions with similar morphology were earlier recorded for the woolly mammoth ribs and vertebrae (Krzemińska, 2009, Figs. 7, 8 and 15; Krzemińska and Wędzicha, 2015; Krzemińska et al., 2015, Figs. 4 and 6; Kevrekidis and Mol, 2016) and referred to as osteolytic changes that could have been caused by trauma, infection, deficiency of vitamins, minerals, or protein, or even tumors (Krzemińska and Wędzicha, 2015, Fig. 3). A similar pattern of lesions was also reported for young (< 20 yr-old) modern African elephant (Haynes and Klimowicz, 2015, Fig. 9). If Krzemińska et al.'s

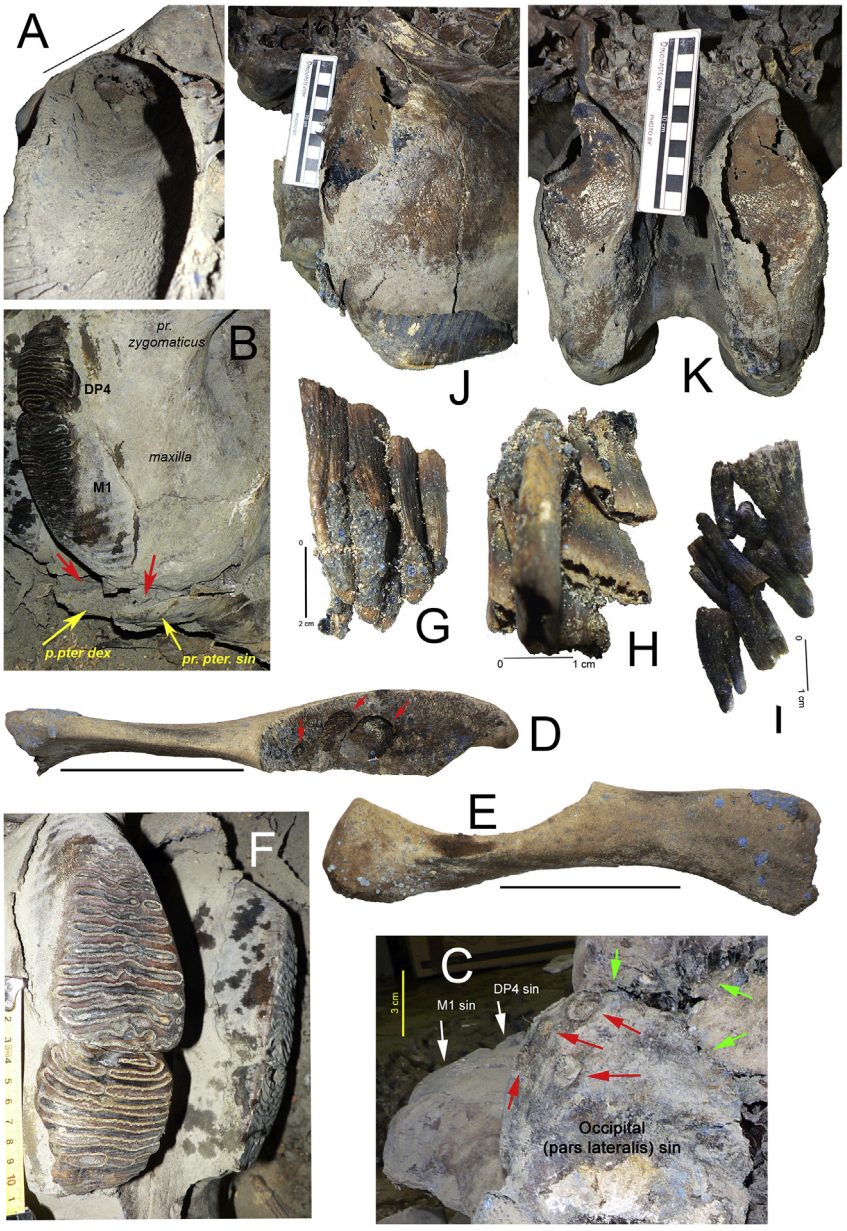

Fig. 8. The Zhenya Mammoth cranium and upper teeth. **A** – the apex surface of the right (normally developed) tusk alveolus; **B** - the upper left DP4/M1 in wear (arrows: yellow - the pterygoid processes forming caudal wall of the M2 alveolus, red – developing cracks between pterigoid processes and maxillae). The photo was taken in spring 2013 (ZIN), when the upper M2 were not yet discovered and extracted; **C** – the occipital side of the cranium, dorsocaudal view (arrows: red - the bone lesions, green – the gaps along fusion lines of the occipital bones); **D** – **E** –the right jugal bone, dorsal (D) and lateral (E) views (arrows: red – three bone lesions on the articulation surface; **F** - the right upper PD4/M1, occlusal view; **G, H** - the right upper underdeveloped M2, lateral (G) and ventral (H) views; **I** - the disintegrated underdeveloped upper left M2; **J** – **K** – the upper dentition with disintegrated walls of the M2 alveoli after the pterygoid processes became detached, lateral (J) and caudal (K) views. Scale 10 cm where not labeled. (For interpretation of the references to colour in this figure legend, the reader is referred to the web version of this article.)

(2015) proposed lesion etiology is true, then it appears that Zhenya's cranial lesions were progressing.

3.3.3.1.2. Jugal bone pathology. Both jugal bones were unfused with the jugal processes of the cranium (Fig. 8, D and E). The left jugal bone of the exposed side of the carcass remained in articulation with the cranium, being supported by skin before the burial, and remained supported by frozen sediments around it until the excavations, after which it became separated. The right jugal fell off the cranium after it was thawed and prepared for mounting in St. Petersburg. This bone generally remains very loose in the cranium until it firmly fuses with the jugal processes of the temporal and maxillary bones. If the carcass had any movement (i.e. carried by flood waters) or physical impacts (trampling by animals or butchering), most of the cranial bones including jugals would have fallen apart and scattered around the carcass before the burial, which did not happen.

There are three shallow round and oval lesions found on the articular surface of the right jugal, which was available for our study (Fig. 8, D and E). The lesions measured 34 × 22 mm, 27 × 14 mm, and 11 × 7 mm. These lesions had similar morphology to the cranial lesions, suggesting that a disease was progressing. A lesion of similar type and size (34 mm × 51 mm) was also reported on the "internal side" of the left jugal bone and described as "small rounded hole." It was reported as being sent for CT scanning to

clarify the “unusual pathology located on the internal side of the bone” (Pitulko et al., 2016; Suppl. Text, p. 6). However, in the text of the main paper, this lesion was interpreted as an “injury” inflicted by an ivory or bone weapon entering from the cheek surface of the mammoth lying on its right side (Pitulko et al., 2016, p. 261). If this had happened, the unfused jugal bone would have been easily disarticulated and shifted away from its joints, which was not observed on the *in situ* cranium. In order for humans to inflict an impact with a weapon to the internal surface of a jugal bone, the bone must be removed from the joints and turned upside down, which seems an irrational action performed on the injured and alive animal.

3.3.3.1.3. Mandible. (Fig. 9, A-K; Supplementary Table S5)The symphysis had a relatively short process. Both hemimandibles had two mandibular foramina. The caudal openings of the mandibular canals (*canalis mandibularis*) were closed by the bony plugs in both hemimandibles. Normally, the closure of this opening occurs after formation of the last molars (m3), when development and growth of the molars comes to an end. The early formation of this “plug” in the Zhenya Mammoth mandible is a very unusual condition and is likely linked to the malformation of the lower molars.

The mandible, which was lying on its side, was found collapsed and broken into two halves at the symphysis area (Fig. 9, G and H). Both half-jaws appeared complete and in excellent condition, with a small area (1.0 × 1.5 cm) of slight deterioration of the cortical bone on the inner side of the left condyle (Fig. 9, A). Unlike the left part of the jaw which became separated from the cranium during excavations to ease access to the cranium, the right hemimandible remained in articulated position being supported by the frozen soft tissues, skin and sediment (Fig. 4, B). Both jaws retained very thin coronoid processes intact (Fig. 9, B and C), one of which (right) was mistakenly reported as broken off (Pitulko et al., 2016). The split mandible and the “broken” coronoid process were interpreted as the evidence of purposeful breakage of the bones by prehistoric humans for tongue extraction (Pitulko et al., 2016).

The mandible's symphysis area demonstrates a “dry” (post-mortem) breakage, with characteristic right angle and rough surfaces (Wheatley, 2008), which unlike “green” breakage could not produce similar appearance if it was broken shortly after the mammoth's death. ‘Dry” breaks typically happen to bones that lose flexibility due to moisture loss, and eventually organic content, becoming fragile and unable to resist applied pressure. In mammoth bones recovered beyond the permafrost area, the fragile condition of bones and their breakage in the symphysis area are especially common. The symphysis area that connects the two dentaries with heavy teeth is relatively narrow, and in a “dry” condition often breaks under sediment pressure. It also often breaks during excavations when the bone is removed from the sediments and not secured in a jacket (Kevrekidis and Mol, 2016; Kevrekidis, pers. comm.). The mandible's symphysis and ascending rami are also prone to very easy breakage if they are trampled (Fig. 9, E and F), such as recorded for the natural trap of the Mammoth Site of Hot Springs in South Dakota (Agenbroad and Mead, 1994).

3.3.3.1.4. Tusk. (Figs. 10 and 11, Supplementary Table S6). Only the right permanent tusk (I) was developed in this individual. It had some damage to the tip and was mostly dark (black) in color, with the surface extensively covered by thin powder of vivianite. The cross section at the alveoli measured 9.3 cm × 8.7 cm, and the tusk's length on the greater curvature was 160 cm. The tusks with similar parameters collected from Siberia would be assigned to males between 25 and 45 years old or females about 33 years old (Vereshchagin and Tikhonov,1986; Tabl.1, Figs. 5 and 6), as based on counts of visible paired light and dark bands and assessment of the curvature lengths. If applied to Zhenya, this method greatly overestimates the age, conflicting with the probable age determined by comparison with African elephant tooth replacement and wear (Laws, 1966).

Proboscidean tusks, especially of males, are characterized by irregular growth and their size depends on nutrition, rate of wear, and dimensional variations across the populations, making reliance on morphological variables problematic for reliable sex determination without independent knowledge of age. Unlike well-developed methods distinguishing sexual dimorphism in modern elephants and mastodons (Pilgram and Western, 1986; Smith and Fisher, 2011, 2013), the methods discriminating sex and age of woolly mammoth tusks remain disputable. The comparisons revealing precise differences in growth rates of tusks between Zhenya and same-aged mastodons is yet impossible. Zhenya did not reach the age of the youngest studied mastodons (16 years and older; Smith and Fisher, 2011). However, it is obvious that the tusk growth rate was significantly higher for Zhenya, exceeding the tusk length in youngest mastodons (estimated 16 yrs-old) by 16.8–41%. The shape of the Zhenya Mammoth tusk is typical for the species, with a deep (about 420 mm) pulp cavity (Fig. 10, B) reaching about 25% of the total length of the tusk and approximately equal to the alveolus length.

The tusk had noticeable bands of alternating dark and light colors, which become obscure towards the distal end (Fig. 10; C and D). These bands or periradicular features were interpreted as annual growth cycles of the woolly mammoth (Vereschagin and Tikhonov, 1986), and based on studies of the Columbian mammoth (El Adli et al., 2015) each couple of light and dark bands were confirmed as “first-order” structures that reflect one year of dentin apposition. On the proximal end of the Zhenya tusk, there are three distinct pairs of bands measuring 6.0, 6.0, and 6.6 cm in width, and that are close to the band length variation (4.0–7.9 cm) of the mature adult Columbian mammoth nicknamed Zed, from Rancho La Brea, California (El Adli et al., 2015). The dark bands that are on average 1 cm wide on the Zhenya tusk are interpreted here as deposited in winters, while light-colored bands, about 5 cm wide, reflect intensive growth of the tusk during summer, the most favorable part of the year. The “summer” bands may also be interrupted by additional dark bands, such as B2 (Y3) that may correspond to natural or physiological stresses. Such stresses observed in African elephants include shortage of food or water, and musth in bulls (Haynes, 1991; Lee and Moss, 1995). The Y3 zone has two dark bands, which we interpret as B1 corresponding to the “normal” depletion of food resources during winter, which is spaced from others within 5–6 cm, and B2 reflecting additional physiological stress that occurred in late spring - early summer. The most proximal dark-colored band corresponding to the last winter of Zhenya's life differs from others by excessively deposited dentin forming a ~10 mm wide torus which slightly protrudes beyond the rest of the surface of the tusk. The proximal light-colored band adjacent to the latter has a noticeably reduced diameter, which is smaller than the preceding light-colored band, making this torus stand out (Fig. 10, C and D). These morphological features are not pathological, but most likely reflect major physiological or metabolic changes in the mammoth during the last year (winter) of his life. The size of the light-colored band at the end of the tusk (Y1) corresponds to those of the completed cycles of Y2 and Y3 and indicates that Zhenya's death occurred between the end of summer and onset of winter, with the latter not yet demarcated by the sharp “first order” boundary. These features place Zhenya's death in fall.

The tip of the tusk is broken off and has several cracks, expanding into a large gash on the ventral side (Fig. 11, A, A′). It is narrow and deep at the tip and widened and shallow proximally. This gash with sharp edges most likely developed during weathering and exposure to elements, before the carcass became buried.

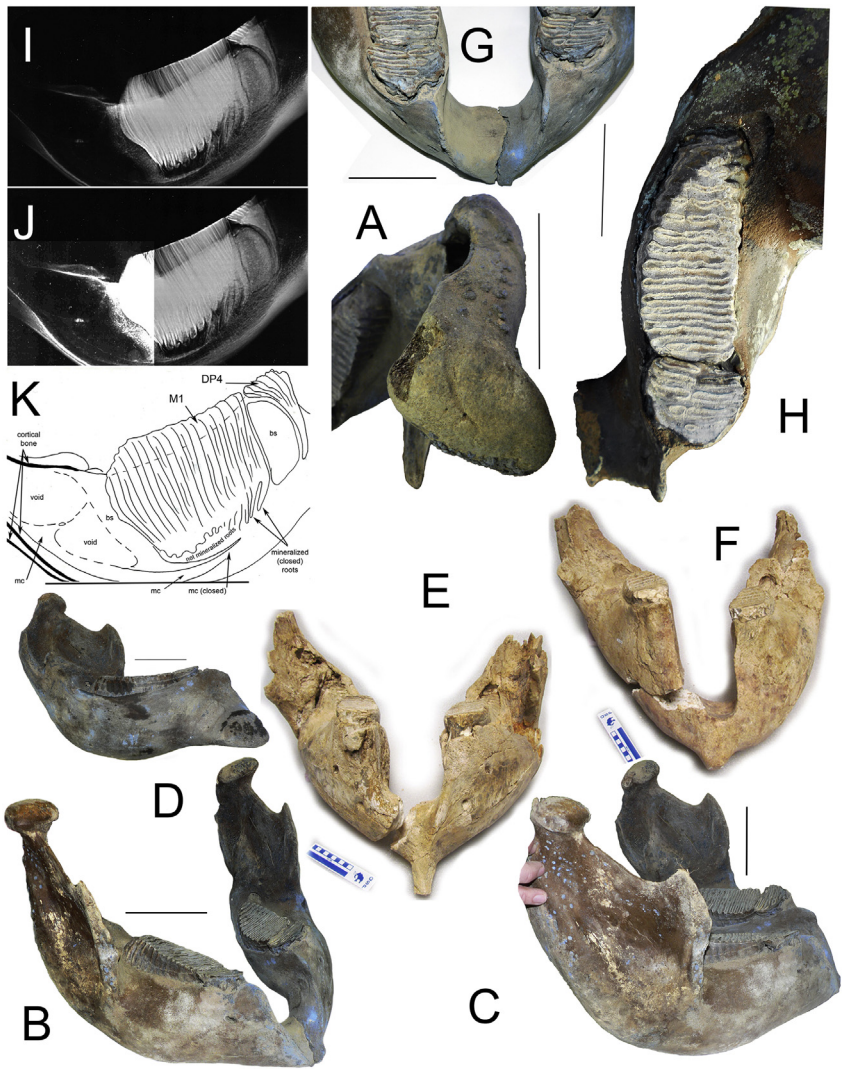

Fig. 9. The Zhenya Mammoth (A-D, G-K) and Columbian mammoth (E, F) mandibles. **A** – the left condyle with the slightly deteriorated ("dry" breaks) surface; **B, C** – the glued together hemimandibles, anterolateral (B) and lateral (C) views; **D** – the left hemimandible with the break surface in the symphysis area, medial view; **E** – **F** - the specimens 83HS190 and MSL 2766 from the Mammoth Site of Hot Springs, SD, Inc. exhibiting "dry" breaks in the symphysis areas; **G** – the symphysis area with the "dry" break line on the caudal surface, dorsal view; **H** – the left hemimandibule with dp4/m1 in wear, occlusal view; **I** – **J** – the X-Ray of the left hemimandible, dorsal views, I – the crown, J – the hollow chamber(s) behind m2; **K** – the sketch with labeled features in I, J, bs – bony septum, mc – mandibular canal. Scale 10 cm where not labeled.

Besides the gash, the end of the tusk has several narrow and shallow longitudinal scars of narrow and long flakes removed from the surface reaching a length of 40 cm and located on the lateral and ventral sides (Fig. 11, B, B'; see also Pitulko et al., 2016; Fig. S4). This flaking pattern is very similar to the broken-off tips of the African elephant tusks collected around water sources and illustrated by Haynes (1991; Haynes and Klimowicz, 2015) (Fig. 11, C–E). African elephants exhibit very aggressive intraspecific behavior over access to water when it is not abundant, and by the end of the dry season multiple tusk tips and shaft fragments can be found at many water sources. The elephants break tusks when shoving each other, and bulls break them when fighting other bulls (Haynes, 1991). The broken-off tips and fragments exhibit a variety of features such as seemingly "prepared" striking platforms, ripple marks, feather terminations, bulbs of percussion, and tang-like shapes, so that they resemble knapped lithic flakes and cores (Fig. 11, C–E) (Haynes, 1988, 1991,). These naturally created forms of broken tusks even have the "triangle" shaped fragments (Fig. 12, E) similar to the pieces discovered at the Berelekh (Vereschagin, 1977) and the Yana sites, which were interpreted as a distinct tusk breaking technology of humans (Pitulko et al., 2015a: Fig. 18, C and D; Fig. 20; Pitulko et al., 2015b: Figs. 16, B and 17). It also appears that the pattern of naturally broken African elephant tusks match experimentally produced breakage on mammoth ivory in low temperatures (Khlopachev and Girya, 2010: Figs. 3 and 4). Haynes (1990) also has pointed out that the broken ivory is never present within the elephant-dug excavations at water sources, indicating the breaks are not the result of using the tusks to dig. Zhenya's tusk cleavages pattern and absence of flakes near its carcass correspond to the behavioral pattern of the African elephant bulls, and indicate that the tusk breakage happened away from the area of the burial.

3.3.3.1.5. Cheek teeth. The Zhenya Mammoth had all erupted cheek teeth in place, identified as DP4/M1 in the upper jaw, and dp4/m1 in lower jaw, based on wear patterns and measured parameters (Fig. 8, B, F, J, K; Supplementary Table S7 and S8). The upper and lower dP4 on the left side retained the last 7 and 4 distal plates in wear, correspondingly. The upper M1 had 18 plates with 11 plates in wear, while the lower m1 had 19 plates with 14 plates

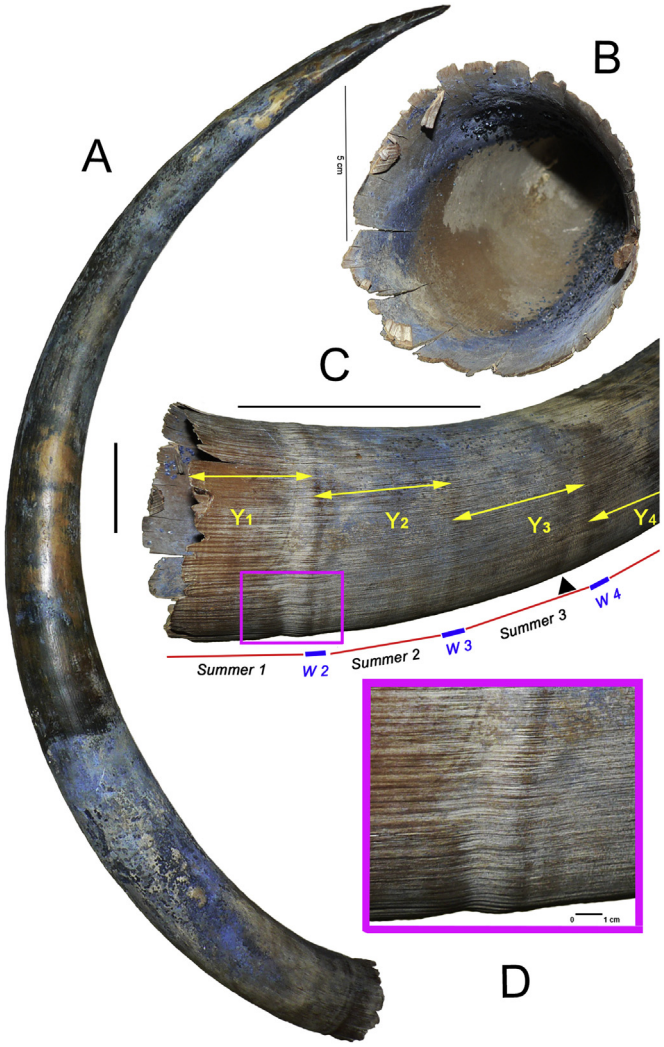

Fig. 10. The Zhenya Mammoth right tusk. **A** – the right tusk, medioventral view, **B** – the pulp cavity, **C** – the proximal part of the tusk, lateral view, Y1-Y4 - the light and dark bands of the last four years (counted backwards) of the Zhenya's life, W2-W4 – last winters of the Zhenya's life, black triangle - intermediate dark ("stress") band of slow growth, magenta square – zoomed out D; **D** – the last dark band on the excessively deposited dentin (exteriorly projected torus) followed by the light band with a groove. Scale 10 cm where not labeled.

in use.

The Zhenya mammoth's un-erupted right and left M2 appeared to be under-developed: the right M2 consisted of the first two enamel plates fused by cementum at the upper part of the crown, and two rows of unfused enamel plates behind them. The largest (2nd) plate of the right M2 measured 34 mm high and 43 mm wide. The left M2 had four rows of plates, which were not fused (Fig. 8, G-I).

The X-ray image of one hemimandible showed that the lower dp4 crown retained the distal mineralized root. The M1 had a crown that was mineralized from the top to the lower edges of the enamel loops, with only few proximal roots closed and mineralized (Fig. 9, I). The mandibular canal was open (functioning) below the roots of the distal half of the M1, and completely closed by the grown-in bone in the mesial portion. Therefore it is likely that all the mesial roots were closed, which is not obvious on the X-ray image (Fig. 9, I, J). The M1 crown is separated from the void behind it by relatively thick bony wall. During normal development of *M. primigenius*, the septa between the M1, M2, and M3 were not complete, and the crowns of these teeth touched each other (Maschenko, 2002). The height of the void is 90 mm, with a length of less than 50 mm. The void seems to be sub-horizontally separated by barely visible and very thin bony septa into two halves, neither of which had traces of teeth (Fig. 9, J and K). Revealed on one side of the jaw, we assume that similar void was present in the other hemimandible. These voids correspond to the upper alveoli, which contained the underdeveloped M2.

The absence of molars or significant underdevelopment has never been reported before for the woolly mammoth. The disproportionately small molars M2 (or their absence in the lower jaw) in the large upper alveoli of the Zhenya Mammoth might have been inhibited by the formation of slow growing benign and non-inflammatory odontogenic cysts or dentigerous (follicular) cysts that form when the tooth fails to break through the gingiva. Once formed, the cyst that is filled with fluid grows, preventing the normal developing of the roots, putting pressure on the surrounding bone that leads to its desorption. This process may continue for decades without causing pain. Eventually the cyst becomes large enough to break through the bone, forming a fluid-filled swelling in the oral cavity that may cause health problems. In humans, these cysts almost exclusively occur in permanent dentition with over 75% of all cases located in the mandible (Dunfee et al., 2006; Som and Curtin, 2003).

Associated with dentigerous cysts is ameloblastoma, which is a locally aggressive benign tumour diagnosed in lower or upper jaws. This hard painless lesion may slowly grow for decades and eventually erode through the bone cortex into adjacent soft tissues. In humans, the "soap-bubble" lesions of the multicystic ameloblastomas accounts for 80–90% of cases (Dunfee et al., 2006; Som and Curtin, 2003) and may be the case of the Zhenya Mammoth's M2 anomaly and the absence of the lower second molars.

3.3.3.2. Hyoids. The majority of the hyoid bones were preserved, including both the stylohyoids, unpaired basihyoid and a large proximal fragment of the right thyrohyoid (Fig. 12). The stylohyoid bones of the right side were found in anatomical position, or *in situ* (Fig. 12, A and B). The stylohyoids had deformed inferior rami (Fig. 12, C-F). The stylohyoid posterior rami slightly differ in shape and size on the left and right bones (Supplementary Table S9).

In Proboscidea, the thyrohyoid and basihyoid are articulated and loosely attached to the stylohyoids through relatively long stylohyoid ligaments that support the tongue and pharyngeal pouch (Shoshani, 2003) posteriorly and are embedded in the tongue muscles anteriorly (Eales, 1926). The stylohyoids are very rigidly articulated with the skull by muscles allowing no movement. In the African elephant, five pairs of muscles (*m.styloglossuss*, *m. hyoglossus*, *m. geniohyoideus*, *m. mylohyoideus*, and *genio-hyoglossuss*) are connected to the hyoid bones. The latter two pairs are especially large, fan-shaped muscles that underline the mouth floor with fibers radiating from the posterior side of the mandibular symphysis anchoring and penetrating deep into the tongue base and connecting it with the anterior border of hyoid and thyrohyoid (Eales, 1926). If the tongue of the Zhenya Mammoth was removed by ancient hunters, as recently proposed by Pitulko et al. (2016), the three large pairs of muscles with the hyoid embedded in them would have been also removed together with at least anterior part of the hyoid complex, the basihyoid and thyrohyoids, which in such case also would have been missing. However, the basihyoid and anterior part of the right thyrohyoid were in place (Fig. 12, G-I); the latter had a split fiber on the end and the left thyrohyoid was not recovered. The right thyrohyoid might have been partly eaten by small carnivores along with the tongue and the supporting hyoid muscles, pharyngeal pouch, esophagus, and larynx, while the left thyrohyoid became loose, detached from the muscles and got lost.

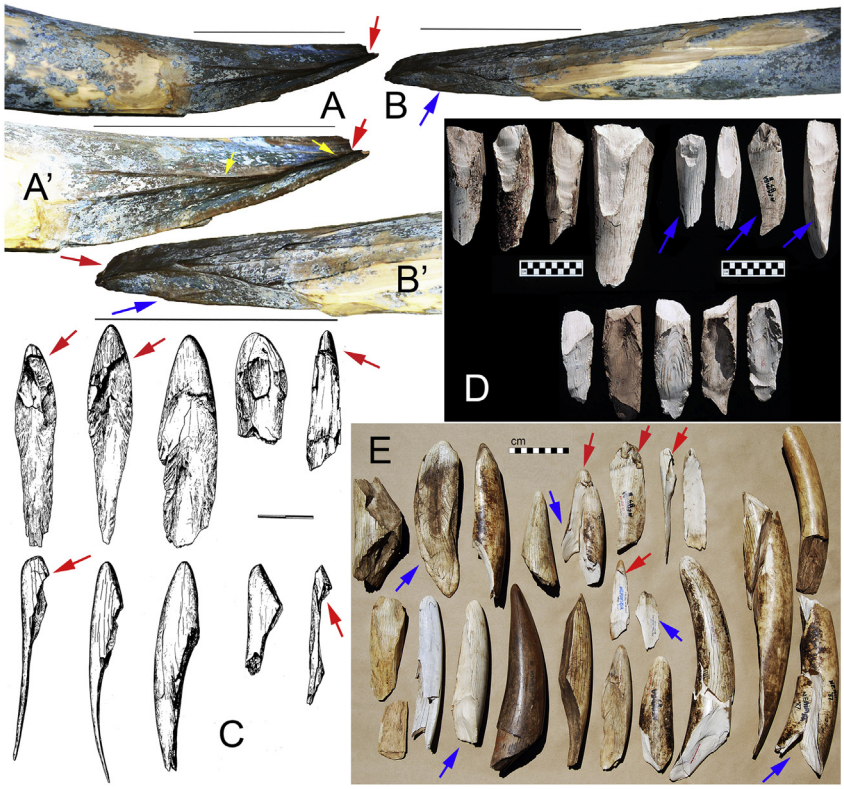

Fig. 11. The Zhenya Mammoth tusk tip compared with naturally broken tips of the African elephants. **A, A'** - lateral, **B, B'** – ventral views; **C** – **E** - the tusk tips broken by African elephants fighting over access to water at single water sources and exhibiting breakages similar to knapped stone flakes (C - the Shabi Shabi seep, Zimbabwe, drawing by M. Bakry), E – Nehimba, Hwange National Park). Arrows: red – the break on the Zhenya's tip matching those of the African elephants, blue – the break of the Zhenya's side of the tip matching those of the African elephants. Photos C-E courtesy of G. Haynes. Scale 10 cm where not labeled. (For interpretation of the references to colour in this figure legend, the reader is referred to the web version of this article.)

Soft tissue decay also could have removed some of these parts.

3.3.3.3. Vertebrae. The total length of the spinal column from the atlas to the distal edge of the fourth sacral vertebra in anatomical position along the curvature was 1947 mm, and 1817 mm long measured along the chord. The cervical vertebral series CI-C7 that included the soft tissues and vertebral discs with cartilaginous tissues between them was 247 mm long. The length of the thoracic segment of the spine along the curve was 1450 mm. The length of the lumbar portion of the spine was 497 mm.

The neural arches were not fused to the centrum bodies and showed a higher degree of suture obliterations in the last vertebrae of the rib cage. The vertebral plates were not fused to the centra. None of the spinous and transverse process apophyses were preserved on the bones, exposing the surfaces of spongy bone covered by papillae.

The intervertebral discs were preserved on all vertebrae. All vertebral plates that were available for examination had cartilaginous rings adjacent to them. The width and thickness of the cartilage tissues had somewhat shrunk during storage of the carcass.

3.3.3.3.1. Cervical Vertebrae (C)

Atlas C-1

There were no visible sutures on this vertebra. The apophysis of the transverse processes had a papillae structure in the fusion and growth zones (Fig. 13, A-D; Supplementary Table S10). The dorsal surface of the neural arch was evenly rounded and had a median eminence. The height of the foramen for the odontoid process was approximately equal to the height of the spinal canal.

Axis C-2

The odontoid process was completely ossified. This process and neural arch were completely fused to the centrum, without a trace of sutures. The caudal vertebral plate was not completely formed (Fig. 13, E-G; Supplementary Table S11). Its thickness in the central part was less than 1 mm, while along the lateral edges it was significantly thicker and varied between 2.5 and 3.0 mm. The plate had few irregularly shaped holes about 1.0–3.0 mm in diameter that were concentrated in the center and along the lateral sides. A few large holes, up to 7.0 × 4.7 mm, were in the center. The holes are nutrient foramina.

The dorsal and ventral parts of the transverse process that form the transverse foramen are completely fused and have a visible suture.

Cervical Vertebrae C3-C7

(Fig. 14, A). The neck vertebrae were preserved with abundant soft tissue holding them together. The central part of the vertebral plates had between 3 and 9 holes with diameters of 0.5–3 mm. All the cervical vertebral plates preserved the dried out intervertebral cartilages between them, which had the shape of ring. The "rings" were about 4.0–5.0 mm thick at their inner edge and reached 12 mm at the lateral side. The spacing (two vertebral plates with cartilage between them) between the 6th and 7th cervical vertebral centra was 9 mm. The dorsal and ventral parts of the transverse process on the C-3 – C-7 vertebrae were not fused and had a deep gap between them on the edges, reaching 4 mm. The ossified apophyses of the transverse processes represented the centers of

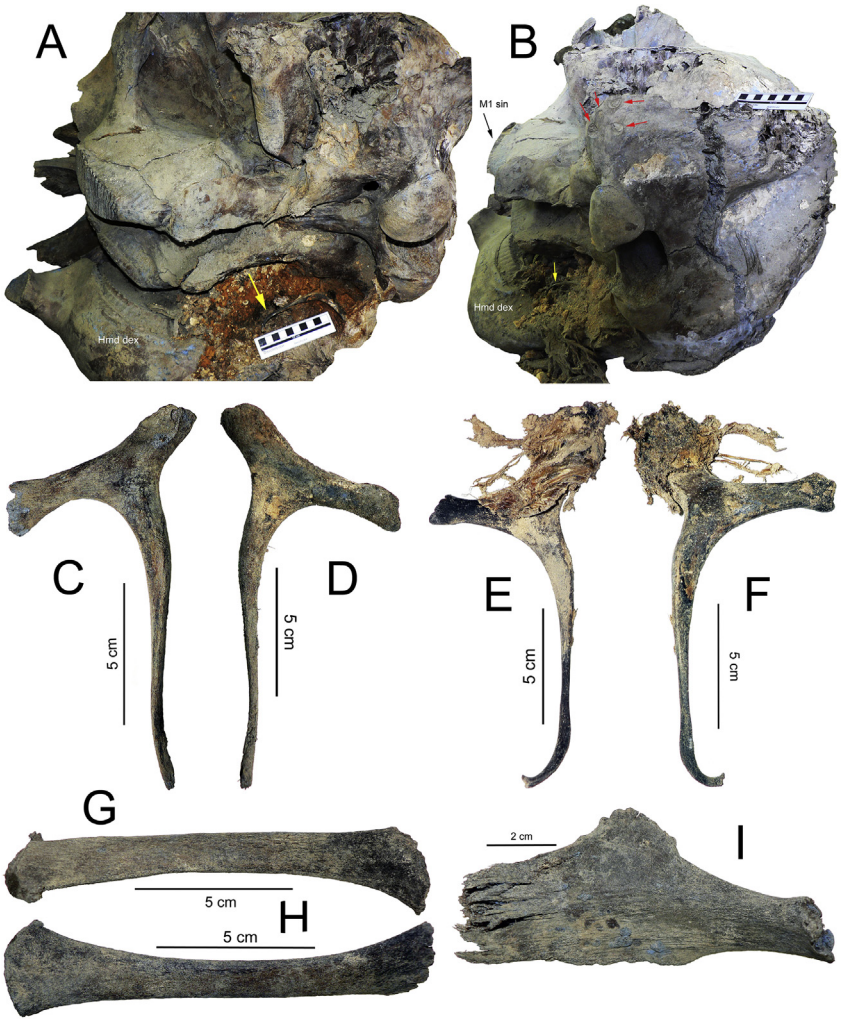

Fig. 12. The Zhenya Mammoth skull *in situ* with the attached right stylohyoid (A, B) and other hyoid bones **(C–I)**. A, B – the cranium with the right stylohyoid (yellow arrows) and hemimandible *in situ* (the left hemimandible is removed), C – lateral and D –medial views of the left stylohyoid; E – medial and F – lateral views of the right stylohyoid with attached tendons; G – cranial and H – caudal views of the basihyoid; I – the proximal fragment of the right thyrohyoid. Red arrows show the bone lesions. Scale 10 cm where not labeled. (For interpretation of the references to colour in this figure legend, the reader is referred to the web version of this article.)

ossification of about 4.0–5.0 mm in diameter.

3.3.3.3.2. Thoracic Vertebrae (T1-T21). (Fig. 14B–F)**.** All apophyses were not completely formed and remained unfused to the vertebrae. The thoracic vertebrae T1-T21 had costal facets for ribs. The last thoracic vertebra, T21, had a medium-sized facet with a diameter of less than 13 mm. All thoracic vertebrae have centra unfused to neural arches, often exhibiting deep gaps between them. The T3-7 had noticeably bent dorsally spinous processes, which have not been observed in other woolly mammoth specimens. Very few of the vertebral plates could be examined from both sides due to complete adherence between plates of the adjacent vertebrae, and all the studied cranial and caudal plates of T3 to T9 had multiple miniscule holes. The plates, which were separated from the centra and had detached soft tissues, exhibited a circular thinning in their middle part approximately 3–4 cm in diameter, speckled by multiple small sized, about 1–2 mm in diameter, nutrient holes of still growing bone (Fig. 14, D). The most cranial thoracic vertebrae had the largest holes. The T2 had very large holes in the central part, 3.8 × 2.0 mm and 3.5 × 1.7 mm. A significant amount of the vertebral plates had very small ridges, exhibiting similar pattern of osteophytes on the thoracic vertebra of a very old African elephant (Haynes and Klimowicz, 2015).

The first few thoracic vertebrae have spinous processes unusually bent ventrally the mid-shafts. The T1 – T7 retained dried out and mummified rings of intervertebral cartilage firmly attached to centra. The width of the rings varied between 0.5 cm and 4.5 cm, with prevailing width around 2–3 cm. The thickness of the ring measured between the T1 and T2 was 7.5 mm.

The caudal side of the distal end of spinous processes had the porous bone texture, which could be due to either active growth of the bone, or early signs of deterioration of the bone structure due to disease. The spinal processes of the T5, 6, and 7 have round or oval hollows at their bases, similar to that recorded in the same vertebral locations on woolly mammoths from Europe and Siberia (Maschenko et al., 2006; Krzemińska, 2008, 2009, Fig. 3, Figs. 4, 5 and 10; Leschinskiy, 2012, Fig. 12 b, c, d; Krezmińska et al., 2015, Figs. 4 and 5), and African elephants (Haynes and Klimowicz, 2015, Fig. 9). According to Krzemińska et al. (2015), these lesions correspond to the class IV of osteolytic changes, and may be caused by organismal metabolic disorders due to malnutrition and following a nutritional deficit of vitamins, minerals, and/or protein. In Zhenya's case, all the detected hollows with smooth edges indicate the bone was remodeling and healing after surviving physiological stress.

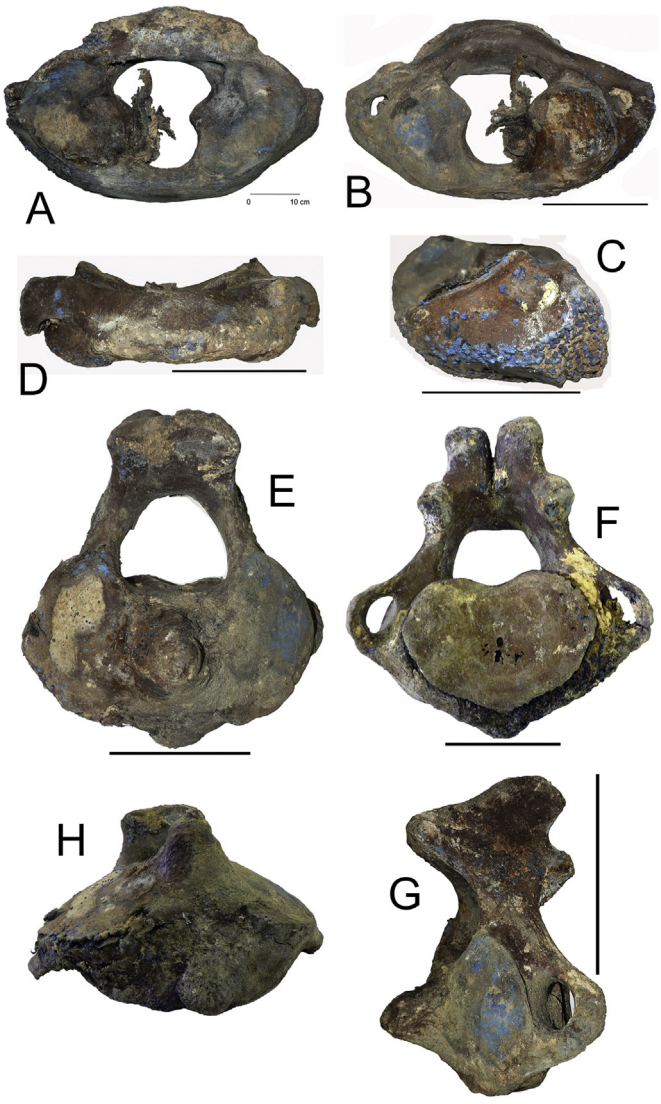

Fig. 13. The Zhenya Mammoth atlas (A–D) and axis (E–G) vertebrae. A and E, - cranial views, C and G – lateral views, D and H - ventral views, B and F - caudal views. Scale 10 cm where not labeled.

3.3.3.3.3. Lumbar vertebrae (L). (Fig. 14G and H). The lumbar vertebrae L1-L5 were characterized by relatively wide and thin centrums, which are typical for this part of the woolly mammoth vertebral column. Large gaps of uncompleted fusions were present between the centrum's body and bases of the neural arches. The vertebral plates had almost completed their growth and ossification, and did not have thinning in their central parts. The L1 and L2 each retained 1 to 3 miniscule nutrient holes in both plates, which were not present on the caudal plate of L3 and the L4-L5 plates. The L1 and L3 had both plates detached, while the L2 had the cranial plate partly fused to the centrum (with fusion line still well visible). The L2 had the spinous process tip broken off and a sign of bone deterioration on the tip of the right transverse process. The L3 exhibited malformation of the left post-zygapophysis and had a "dry" break of the tip of the right transverse process.

3.3.3.3.4. Sacrum (S). (Fig. 14 J and K). All the sacral vertebrae were evenly covered by vivianite powder on the outer and fusion surfaces with distinct papillae of the centrums. Four S1-S4 were not fused with each other and most of the vertebral plates, and were easily detached during the studies, a condition shown earlier for young woolly mammoth individuals (Maschenko, 2002). The transverse processes also were not fused with each other and did not form sacral wings. The S1 centrum retained the fusion lines with the neural arch. Its cranial plate had a lesion in a form of a hole ~0.5 cm in diameter with even walls. The caudal plate has a rough surface covered by multiple miniscule ridges dispersed concentrically and semi-concentrically. This pattern was similar to that of the caudal plate of thoracic vertebra of a very old African elephant, which was identified as having osteophytic margins indicative of ossification of the intervertebral cartilage and arthritis disease (Haynes and Klimowicz, 2015). A similar pattern occurs on the cranial plate of the S2, and the caudal plate on S4 with lesion holes along its ventral edge. The S4 caudal plate did not detach.

3.3.3.3.5. Caudal vertebrae (Ca). Eight caudal vertebrae were recovered with the carcass. The neural arches, vertebral discs, and all apophyses were not fused with the vertebral body.

3.3.3.4. Ribs (R). None of the apophyses were completely ossified and thus were unfused to the ribs. Their surfaces were not completely formed and were covered by a layer of *substantia compacta* (Fig. 15; Supplementary Table S12, 13). Exposure to the air and drying in storage, might have affected some of the ribs (R14-R20) acquiring unusually bent shapes. Similar deformations of mammoth ribs are rarely found and the only case is reported from the Kraków Spadzista street site (Krzemińska and Wedzicha, 2015; Fig. 4). The R1-R16 rib apophyses had two facets divided by a groove, for attachment to two vertebrae, while R17-R21 rib apophyses had single facet for attachement to single centra.

3.3.3.5. Sternum. The sternum was preserved as a single unit, located inside dense connective tissue (Fig. 16). Its length was 445 mm. A large number of ligaments were attached to the cranial and caudal ends of the enclosing connective tissue. The frontal ligaments were directed dorsally, encasing the base of the first pair of ribs in the connective tissue. The thickness of the connective tissue between the first rib and anterior segment of the sternum (presternum) was about 10 mm, while its thickness in the remaining sections was about 3–4 mm. The bases of the second and third ribs attached to the sternum's facets were covered by connective tissue.

Removal of the connective tissue covering the sternum showed that all three ossified segments (presternum, mesosternum, and xiphisternum) lacked a compact layer and had thick cartilage on the ends. The facets of the second and third ribs are located on the contact zone between the presternum and mesosternum and xiphisternum, respectively. The facets of the fourth ribs were located on the caudal edge of the xiphisternum. The facet of the first rib to the mesosternum cranial edge area was much smaller than the area of the distal edge of the first rib. Its length was about 25 mm. Other ribs do not have direct contact with these elements of the sternum.

The sternal facet for the first rib was about 25 mm in length. Other ribs did not have direct contact with the sternum.

3.3.3.6. Pectoral girdle and forelimb. All the epiphyses of the forelimb bones were ossified but remained completely unfused to diaphyses, as revealed during preparation of the bones for the skeletal mounting (Supplementary Fig. S2-S4).

3.3.3.6.1. Scapula. The right scapula was complete and the left scapula had the cranial edge broken off (Fig. 17; Supplementary Table S14). The dorsal apophyses that were not fused to the scapular bodies were preserved on both scapulas being covered by connective tissue. The cartilagenous apophyses were ossified only at their apices. The sizes of the scapular left dorsal apophyses are as follows: the maximum mediolateral diameter (thickness) -

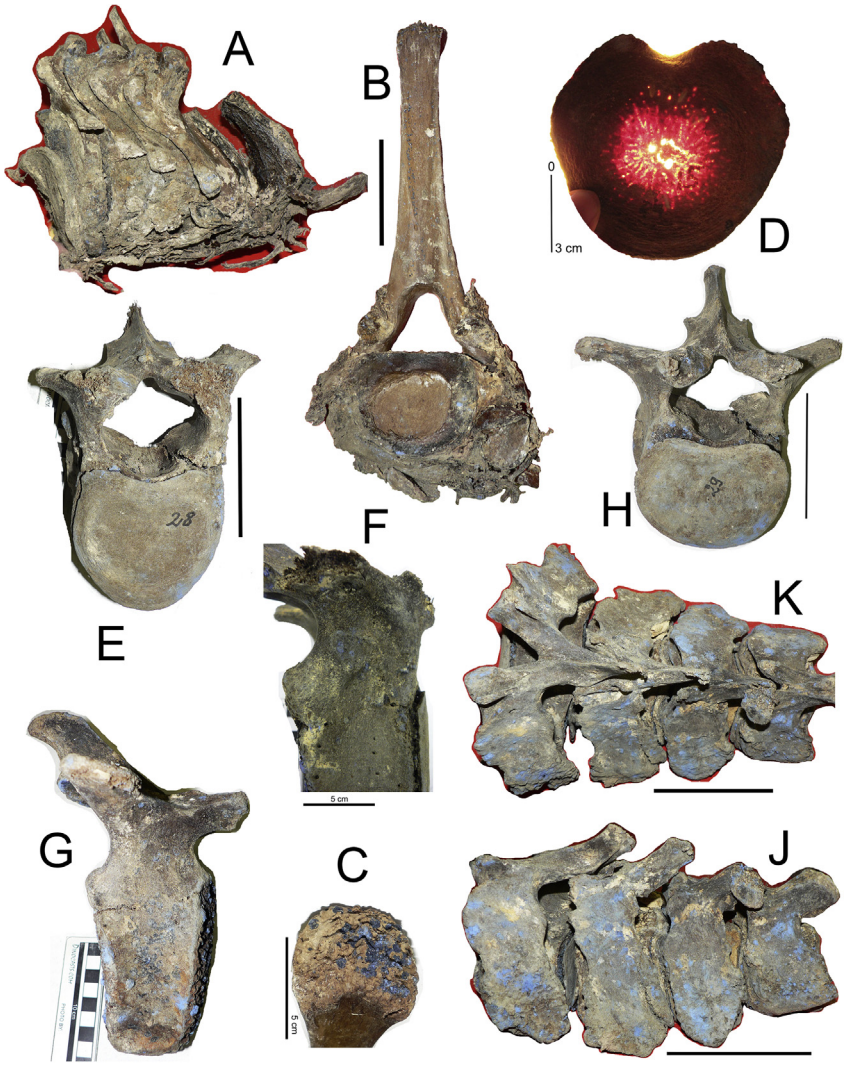

Fig. 14. The Zhenya Mammoth cervical (A), thoracic (B–F), lumbar (G, H), and sacral (J, K) vertebrae. A – the right side of C3-C6 covered by soft tissues, B – T-2 (caudal view), C – the dorsal surface of the T-2 spinous process, D – the T-2 cranial vertebral disc with thinned and perforated central part, E – T-21, cranial view, F – T-21, right lateral view (with a facet for rib); G – L-1, right lateral view; H- L-1, cranial view, J, K – the sacral unfused vertebra (J – left lateral, K - dorsal views). Scale 10 cm where not labeled.

79.0 mm, the maximum craniocaudal diameter - 161.0 mm, the height at the midline - 56.0 mm. Both scapulae had an oval nutrient hole at the base of the proximal part of the scapular spinal process, with a size of 4.5 × 3.2 mm.

The left scapula had a hole with irregular edges along an extensive transverse crack in the scapular spine (Fig. 17, F). The cracked and deteriorated thinned bone exposed the randomly jagged edges. Such condition is characteristic of "dry" breaks and cracks in open air (Chaplin, 1971; Behrensmeyer, 1978). The proximal part of the scapular blade had few very small and shallow spots of cortical erosion. These had uneven shape and superficial cracking around them, caused by the initial stages of cortex deterioration, which is Stage 1 of weathering in Behrensmeyer (1978). There is no evidence that this hole and cortical deterioration had been inflicted by human weaponry or other artifacts as proposed by Pitulko et al. (2016).

3.3.3.6.2. Humerus. (Supplementary Table S15). The proximal and distal epiphyses were not fused to the diaphyses, had deep fusion sutures, or had fallen off the diaphyses (Fig. 18A–E). In African elephant the distal epiphysis of humerus fuses earlier than others and in males it happens, when they are 18 years old, about 3–4 years later than in females (Haynes, 1991). The apophysis of the lateral epicondyles was also not fused to the diaphyses, a feature that has never been observed in known skeletons or isolated bones of this species (Fig. 18, E). The main nutritional foramen on the left humerus measured 11.0 mm tall and 4 mm wide, and was located on the cranial side the diaphysis, approximately 70 mm above the level of the lateral epicondyle.

3.3.3.6.3. Ulna. (Supplementary Table S16). The proximal apophyses on the olecranons and distal epiphyses were unfused with the diaphyses, a characteristic which suggests that Zhenya was younger than 31 AEY (Lister, 1999) (Fig. 18, F-H). The compact layer of the distal end of the diaphysis of the examined left ulna was fully formed, leaving virtually no nutrient holes on the lateral surface. Considerable number of nutrient foramina were located along the base of the distal epiphysis.

In young woolly mammoth specimens, the ulna and radius are connected by ligaments, while in mature individuals these bones begin to fuse along the diaphyses, and in very old individuals the distal ends are fully fused. The Zhenya Mammoth radius and ulna were unfused along their entire lengths.

3.3.3.6.4. Radius. (Supplementary Table S17). This is the only

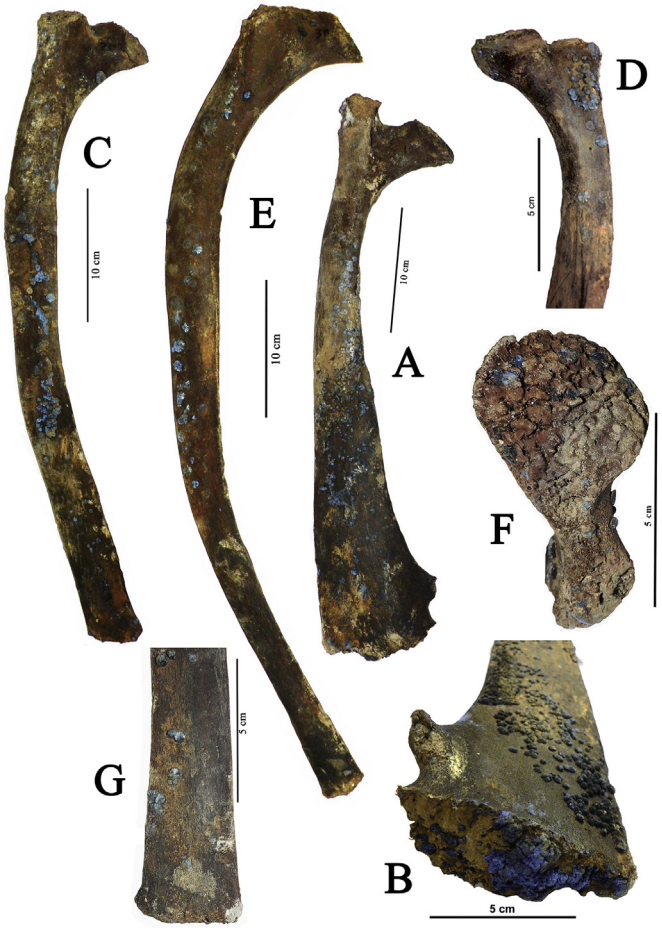

Fig. 15. The Zhenya Mammoth ribs. A – R1 dex (craniolateral view), B – the distal end of R1 sin (craniomedial view), C – R2 dex (craniolateral view), D – the proximal end of R2 sin (craniolateral view), E – R3 dex (craniolateral view), F – the proximal end of R3 dex (dorsal view), G – the distal end of R3 dex (craniolateral view).

element among the long bones of the skeletons which had proximal epiphyses fused with the diaphyses, with complete obliteration of the suture. The diaphyses had well-developed ridges for ligaments along the caudal surface and a ridge on the cranial upper part just below the epiphyses (Fig. 18, I-L).

3.3.3.7. Pelvic girdle and hind limb

3.3.3.7.1. Pelvis. The pelvis was represented by the left and right innominate bones not fused at the pubic symphysis and also unfused to the sacral vertebrae (Fig. 19).

The continuous ilium apophysis was not formed on each innominate and consisted of two separate centers of ossification at the medial and lateral edges of the ilial wings. The apophysis of the right iliac tuberosity (tuber coxae) was 132 mm long and 23 mm wide. The ossified apophysis of the medial corner of the ilium wing (Fig. 19, B) was 223 mm long and 39 mm wide. The pubic bones were not fused and their contacting surfaces were covered by dense, and conical, bony papillae. The cartilage or soft tissue remnants of this contact zone were not preserved (Fig. 19, C). The maximum horizontal width of the pelvic girdle was 1215 mm, and the length of the pubic symphysis was 395 mm.

3.3.3.7.2. Femur. (Supplementary Table S18). Each of the 2 femora had a proximal epiphysis with two separate apophyses unfused to the diaphysis, the head (*caput femoris*) and large trochanter (trochanter major; Fig. 20, A-C), and the distal epiphysis.

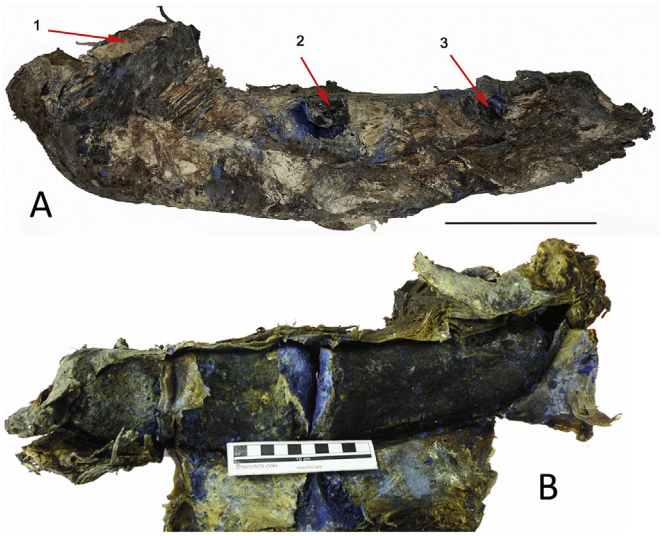

Fig. 16. The Zhenya Mammoth sternum. A – the sternum encapsulated into a connective tissue tegument (left lateral view), B - the sternum with the removed tissues exposing the bones (right lateral view), 1- facet for the 1st rib; 2 - facet for the 2nd rib; 3 - facet for the 3rd rib. Scale 10 cm.

Substancia compacta at the distal epiphyses was very thin and was completely covered by soft tissue. The lateral condyle of the left femur had damage on its lateral wall. The cranial part of the lateral wall is gone, and a deep, round cavity was created inside the condyle. The state of preservation and the pattern of damage indicates utilization of the bone by small scavengers before complete burial of the carcass.

3.3.3.7.3. Tibia and fibula. (Fig. 20, D-H; Supplementary Table S19 and S20). The degree of formation of *substancia compacta* on both tibia epiphyses was higher than on the femur's epiphysis. The fibula's proximal and distal epiphyses were detached.

3.3.3.8. Feet. (Fig. 21). The forefeet (Figs. 5; C and 21, A. B) and hind feet (Fig. 21, C-H) retained soft tissues and skin from the soles to carpals and tarsals. All of the feet but the right manus were found detached from the carcass.

3.4. Taphonomy

The Zhenya Mammoth carcass was found lying on its right side, which preserved most of the skin and soft tissues on the thorax, head, forelimb, and breast. The skin and soft tissues of the left side of the body, including the proximal limb bones, were almost gone, with remnants of muscles and tendons confined to few areas: the dorsal portion including the withers and spine, the proximal half of the frontal part, and the proximal parts of the ribs of the rear end of the torso. The *in situ* body was positioned at ~5° angle facing north, with the hips about 25–30 cm higher than the head and in line with the inclined sediment layers within this bed (Maschenko et al., 2014a, b). The low head position probably contributed to its limited access by scavengers; however, the cranial bones became broken by weight of the accumulated sediments, which continued supporting the cranium in its original shape until the excavations.

The *in situ* articulated position of the stylohyoid and the recovery of almost all parts of the hyoid complex indicate that the tissues surrounding these bones (tongue, esophagus) were not removed in one piece after the mammoth's death, but either slowly deteriorated, or were gradually eaten by small scavengers. The

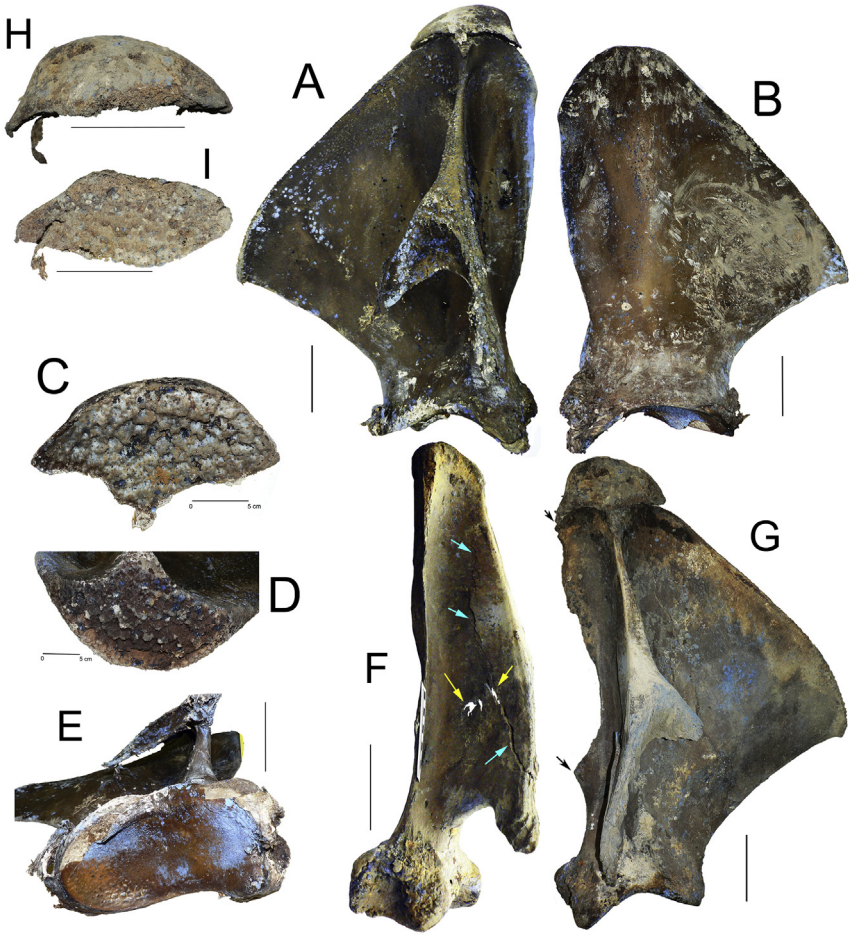

Fig. 17. The Zhenya Mammoth right (A-C, E, H, I) and left (F, G, D) scapulae. A – lateral view; B - medial view; C, D – the fusion surfaces for dorsal apophyses; E – ventral view; F - cranial view, the "dry" cracks (blue arrows) connect the holes (yellow arrows) of deteriorated bone; G – lateral view, the broken off cranial margin is between the black arrows, H - the unfused dorsal apophysis (lateral view); I - the unfused dorsal apophysis (ventral view). Scale 10 cm where not labeled. (For interpretation of the references to colour in this figure legend, the reader is referred to the web version of this article.)

hyoid complexes are often found in complete skeletons of ancient elephants, which were quickly preserved, preventing access to scavengers (Agenbroad, 1994; Agenbroad and Mead, 1994; Kevrekidis and Mol, 2016).

The completeness of the skeleton and the large amount of soft tissues remaining on the carcass indicate that preservation occurred in very specific conditions. It is known that fast burial in anaerobic conditions accompanied by water-related sedimentary processes prevents postmortem disturbance of carcasses by scavengers and other processes such as animal trampling (Behrensmeyer, 1988; Behrensmeyer et al., 2000). However, the burial of Zhenya was not immediate: the mammoth did not die by sinking into a mudhole or river bottom. After the mammoth death, its submersion in floodwaters apparently took place multiple times until the carcass became completely covered by sediment. The proximity of the mammoth's burial to the Yenissei River provided deep and long-lasting submersion of the carcass in the water during these floods. After the mammoth's death in the freezing temperatures of Arctic fall, the carcass became available for a short period to scavengers, before it froze solid. The scavengers, which were possibly wolverines, Pleistocene wolves, or cave hyenas, opened the body's left flank and consumed most of the torso's soft tissues, internal organs, and possibly the trunk. The fragment of the colon with ligaments at the anus opening and complete penis in the caudal part of the body remained out of their reach. The preservation of these parts of the internal organs and tissues suggest that the mammoth was not killed by cave lions or cave hyenas, which would have opened the body from the rear end in a manner similar to their African relatives (Haynes and Klimowicz, 2015: 21; White and Diedrich, 2012). The missing distal phalanges of the right hind sole may have been removed by small scavengers, or by larger carnivores such as wolf or cave hyena. Most likely, the body became frozen and protected by its thick skin, which was too tough for consumption by any size of scavengers. A similar scenario was proposed for the mummy of the steppe bison (Blue Babe) killed by the cave lions in Eastern Beringia (Alaska) (Guthrie, 1990). The carcass of this bison, with skin that was significantly thinner than that of mammoth, was only partly utilized before being abandoned by cave lions when it froze solid. Unlike Blue Babe, the Zhenya Mammoth preserved almost all of its skeletal elements undamaged by scavengers. Considering the multiple but relatively limited modifications to the soft tissue and bones, it is probable that these were inflicted when carnivores such as hyenas or wolves encountered the carcass some time after its death, again an indication the carnivores did not kill the mammoth.

After the corpse became solid frozen, it is unlikely that its completeness and extent of damage changed much until the following warm periods. In spring, floodwaters would have thawed the exposed side of the corpse gradually leading to decay and destruction of remaining soft tissues on the left side of the body,

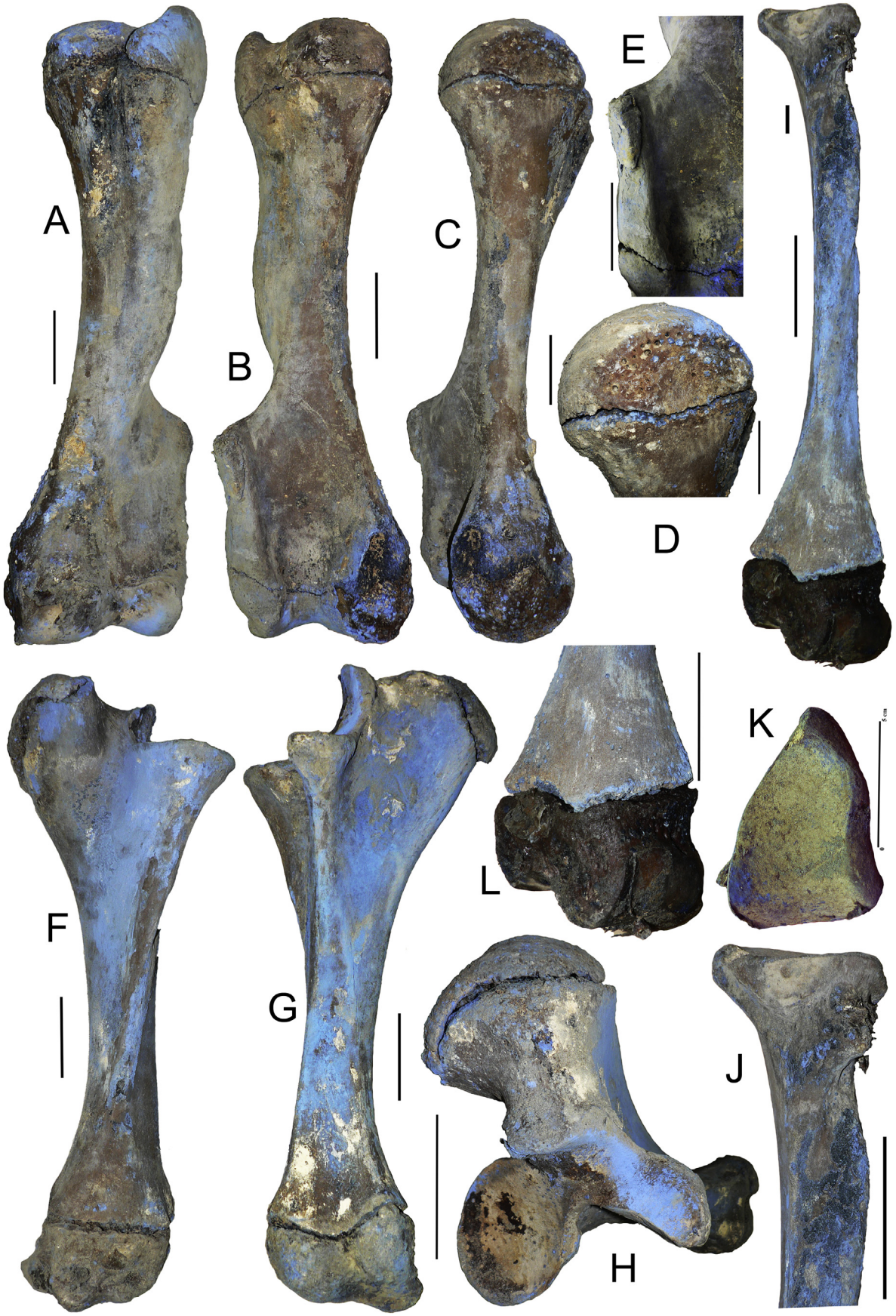

Fig. 18. The Zhenya Mammoth left humerus (A–E), ulna (F–H) and radius (I–L). A – cranial view; B – caudal view, C – medial view; D – the left humerus head (medial view); E – the unfused apophysis of the epicondyle (caudal view); F - lateral view; H – proximal view; G – medial view; I – mediocaudal view; J – the proximal end, caudal view; K – the proximal epiphysis, mediocaudal view. Scale 10 cm.

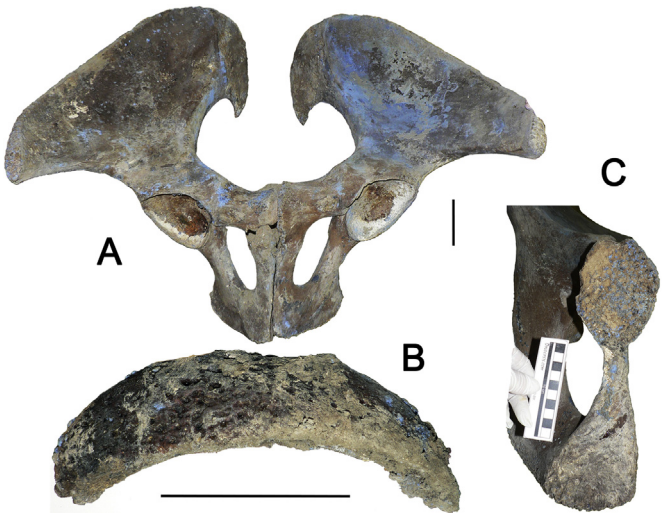

Fig. 19. The Zhenya Mammoth pelvis. A – the unfused innominate bones (ventral view), B – the ossified ilium apophysis (dorsal view), C – the articulation surface of the symphysis of the of the right innominate (pubic and ischium). Scale 10 cm.

and filling the thoracic and abdominal cavities with fine river deposits. Most of the head and the proximal part of the tusk, which were lying downslope, were covered by floodwater sediments during the first spring after the death, but the tusk tip remained exposed to the air and its varying temperatures of four seasons, developing the deep split (Fig. 11, A, A′) and breaking off, until it became completely overlain by the sediments. During very short and cold arctic summers, the lower (right) side of the body remained unthawed preventing complete decomposition of the hide, while the left flank with the opened body cavity, softened skin, and upper limb tissues again became available to scavengers. It is likely that as soon as the first summer after Zhenya's death the hide on the left side became sufficiently deteriorated to expose the distal femur, which was gnawed by small scavengers.

3.5. Ancient DNA

Of the two samples processed for ancient DNA, only the bone fragment provided sufficient quantities of DNA for analysis (Fig. 22; Supplementary Table S21); 7.9% of recovered reads mapped to the mammoth reference genome. Following in-solution target enrichment, we generated a complete mitochondrial genome from this specimen to 7.8x coverage. Sites that were not spanned by at least three independent fragments with the same nucleotide were called as N; the final consensus sequence (GenBank KY454846) has 11.6% (1942bp) unknown nucleotides.

The Zhenya mammoth mitochondrial genome is 99% identical to that of another woolly mammoth, baby Lyuba, which was recovered from a geographically proximate location. Phylogenetic analysis shows strong statistical support for Zhenya's mitochondrial lineage within the clade III/haplogroup B (Fig. 22, S9, S10). This is a deeply diverging lineage of mammoths found mostly in the European part of Eurasia.

4. Discussion

4.1. Zhenya's ontogenetic age

When compared to the Yuribei Mammoth (Dubrovo, 1982), the Zhenya Mammoth appears to have less advanced tooth progression and wear, and therefore is younger. The Yuribei Mammoth had the fully erupted crowns of M1/m1 with the first plates in wear. On the mandible, the first 4 unworn plates of m2 are visible through the small alveoli openings behind M1. This molar progression on the Yuribei Mammoth corresponds to XI age group designated in African elephants by Laws (1966), indicating 15 (± 1) AEY, which may be tentatively calibrated to 13 AEY (Haynes, 2017: Fig. 1) based on recent revisions of the Laws scheme. Direct comparisons with the Asian elephant are limited because the data are unavailable about dental wear of individuals less than 8 year olds, although information is available for 13 year olds (Roth and Shoshani, 1988). It is obvious that the Yuribei Mammoth with an initial stage of wear of the M1 is few years less advanced than that of a 13 year old Asian elephant with the last 9 plates (out of 14–17 plates) in wear, followed by the first 2 plates in wear of emerged M2. These data place the Yuribei Mammoth within the 10–12 AEY age group defined by Laws (1966), or a little older.

The Zhenya Mammoth appears to be older than the Yuka Mammoth, which was aged at 6–8 years (Maschenko et al., 2012). Yuka has the last 4 plates of the dP4/dp4 in wear, and 9 proximal plates in wear out of 16 plates on the M1/m1 crown, which corresponds to the IX stage, or 11.5 AEY old. Haynes 2017 would assign the Yuka Mammoth to 9 AEY. Roth and Shoshani (1988) describe a 5 year old Asian elephant individual having in wear about 20–69% of the DP3/pd3 and 60–70% of the DP4/pd4 plates, whereas a 13 year old has in wear about 75% of the M1 plates and 10–12% of the M2 plates; these are the closest available to Yuka's dental stage and age. The tooth wear of the Yuka Mammoth places it slightly younger that the calculated average age between 5 and 13 year old Asian elephants, which would suggest 7–8 (± 1) years old. Zhenya, with the retained DP4/dp4 and about half the plates in wear on M1 is significantly less advanced in age than a 13 year old Asian elephant with shed Dp4/dp4 and last 9 plates (out of 14–17 plates) in wear on M1 and first 2 plates in wear on M2.

Thus, the tooth progression and wear place the Zhenya mammoth between the older Yuribei Mammoth and younger Yuka Mammoth in age, suggesting 8–10 (± 1) AEY or somewhat older.

4.2. Size and body mass

The Zhenya Mammoth shoulder height was initially calculated by measuring the distance on the carcass between the withers and sole, along the bent elbow and wrist (Supplementary Table S3). However, measurements of extant elephants in lying and standing positions shows divergent results, due to the different distribution of the weight, and in males the discrepancy is on average 15% (Shrader et al., 2006). In addition, the state of the mummified frozen corpse may add bias by affecting how soft tissue compresses or stretches. In fossil and modern Proboscideans, the shoulder height (SH) and body mass (BM) are often calculated by measuring mounted specimens, many of which have incorrectly positioned the vertebral border of the scapulae below the thoracic spinous processes, or place mounted hindfeet in “tiptoed” stance, making the skeletons look taller (Larramendi, 2016). While for museum exhibits it is a widespread practice to mount larger-looking specimens, use of the SH data for actual specimen height and BM may give overestimated results (Larramendi, 2016). The linear relationships between the bone sizes and SH, as suggested by Garutt (1964) (32.2% for humerus and 21.4% for tibia), implies that at birth the animal had a weight = 0 kg, and continues growing with the constant speed to infinity, which also may provide either underestimated or overestimated reconstructions. Unreliable results could be also produced by application of regression equations for

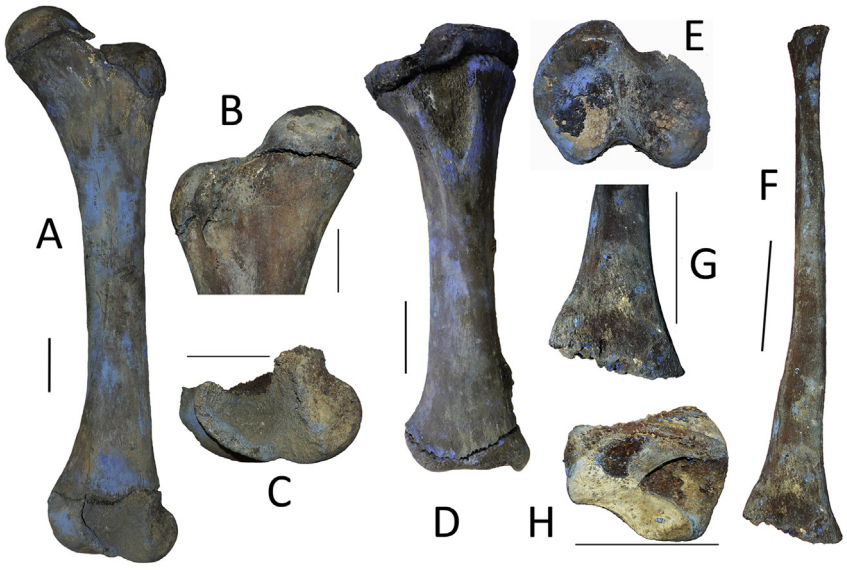

Fig. 20. The Zhenya Mammoth left femur (A–C), right tibia (D, E) and left fibula (F–H). A – laterocranial view, B – the unfused head (caudal view); C – the distal epiphysis (medial view); D – cranial view; E – proximal view; F – medial view; G – the distal epiphysis (medial view); H – oblique-medial view. Scale 10 cm.

calculating the heights of fossil Proboscidea (Lister and Stuart, 2010; Nikolskiy and Pitulko, 2013) simplifying the actual mode of the curvilinear growth of extant elephants. For calculating the Zhenya's shoulder height, we used the method based on measurements of each isolated limb bone (articular lengths of the scapula, humerus, radius, and manus), the sum of which multiplied by 0.98 would give the skeletal shoulder height (sSH, our term) (Larramendi, 2016). In Zhenya's case, based on the articular sizes of the limb bones (Supplementary Table S14-S18), the sSH will be 216.6 cm and this size should correspond to a correctly articulated and mounted skeleton. For adding "flesh" (soft tissues, skin), a factor of 1.055 calculated by Larramendi (2016) would reconstruct the "live" or physiological shoulder height (pSH, our term) to 228.5 cm. Osborn (1942) proposed increasing the Proboscideans' skeletal height for added flesh by 6.67%, which would make the Zhenya's live shoulder height 231 cm. Roth (1990) suggested that addition of flesh in large (sSH over 300 cm) elephants should be not more than 5%, which would add 10.8 cm to Zhenya's sSH, resulting in pSH 227.4 cm. Considering Zhenya's young age and gracility typical for young animals, we conservatively consider the height of 227.4 cm to be the best estimate for Zhenya's live shoulder height.

In relation to average pSH of modern Asian elephants, Zhenya is about 5% shorter than adult females (240 cm) and 18% shorter than adult males (275 cm; Sukumar et al., 1988), as well as 12.5% and 29% shorter than the average adult African elephant females (260 cm) and males (320 cm) correspondingly (Larramendi, 2016). Within its own species, Zhenya's body height is well below the height of adult males. Zhenya is 27.6% shorter than that of 45–50 AEY old Adams Mammoth (Averianov, 1996; pSH 314 cm computed by Larramendi, 2016), 17% shorter than the ~50 AEY old Yukagir Mammoth (pSH 274: Larramendi, 2016), 16.1% shorter than 45 AEY old Berezovka Mammoth (Averianov, 1996; pSH 271 cm by Larramendi, 2016), and 11.9% shorter than the 50 AEY old adult male from the Sevsk Site (Maschenko, 2002, 2006; pSH 258 cm: Lister and Stuart, 2010; Larramendi, 2016).

When compared to woolly mammoth females, Zhenya appears to exceed the body sizes of at least two female woolly mammoths with known age and preserved complete skeletons. Zhenya's is 10.1% larger than 30 AEY old female Chekurov Mammoth (Boeskorov et al., 2009; M2 in wear), which was 223 cm tall (pSH) and its fused epiphyses on the proximal ends of humerus and femur indicate the final stages of the bones growth. Zhenya is also 2% larger than the 60 AEY female Sanga-Yuryakh Mammoth (pSH 232 cm; Larramendi, 2016), but barely larger (0.4%) than the 35–40 AEY old female Kastatyakh Mammoth (M2/M3 in wear; Kirillova et al., 2012), with pSH 226.5 cm.

However, Zhenya is about 1% smaller than the 10–12 AEY Yuribei Mammoth (sSH 227.8 cm; Dubrovo, 1982), with a pSH of 239.2 cm following Larramendi (2016).

For calculating Zhenya's weight, we avoided using the allometric formula of Christiansen (2004) based on five captive modern elephant specimens, because its leads to high errors and overestimates results (Larramendi, 2016). Instead, we applied the equations for body mass (BM) estimation specifically developed for the woolly mammoths based on the von Bertalanffy curvilinear growth function derived from data on extant elephants, producing a low average prediction error (Larramendi, 2016, Table 7). Zhenya falls within the "young forms" (Grade I = $0.000354*SH*e^{2.903}$) north Siberian woolly mammoths, with the result of 2459 kg. The calculated average weight for Zhenya would not be complete without the hair mass (BMH). Musk-ox hair appears to have closest parameters to the woolly mammoth, with its density and weight of about 4 kg/m^2 (Larramendi, 2016). Multiplying it by the 17.2 m^2 of surface area of the Asian elephants weighing up to 3 tones (Larramendi, 2016) resulted at about 68.8 kg for the hair coat. Since Zhenya's weight is about 400 kg lighter than that of a 3-ton elephant, we proportionally scaled it down to 60 kg. Added to the Zhenya's BM (2459 kg), the average BMH resulted in about 2519 kg.

Zhenya's bones have unfused cranial sutures, unfused epiphyses and apophyses in the axial and appendicular skeleton (excluding the feet bones), and uncompleted formation of the vertebral plates, corresponding to a very young individual. If compared to modern forms, Zhenya reached the body size corresponding to 13 year old male African elephant (pSH 225–230 cm) based on the predicted growth function derived from sex- and age-specific data on over 300 free-range young African elephants (Shrader et al., 2006). Based on these data, the average size of the 8–10 year old African elephant (sSH 185–210 cm; Shrader et al., 2006) is 30 cm shorter

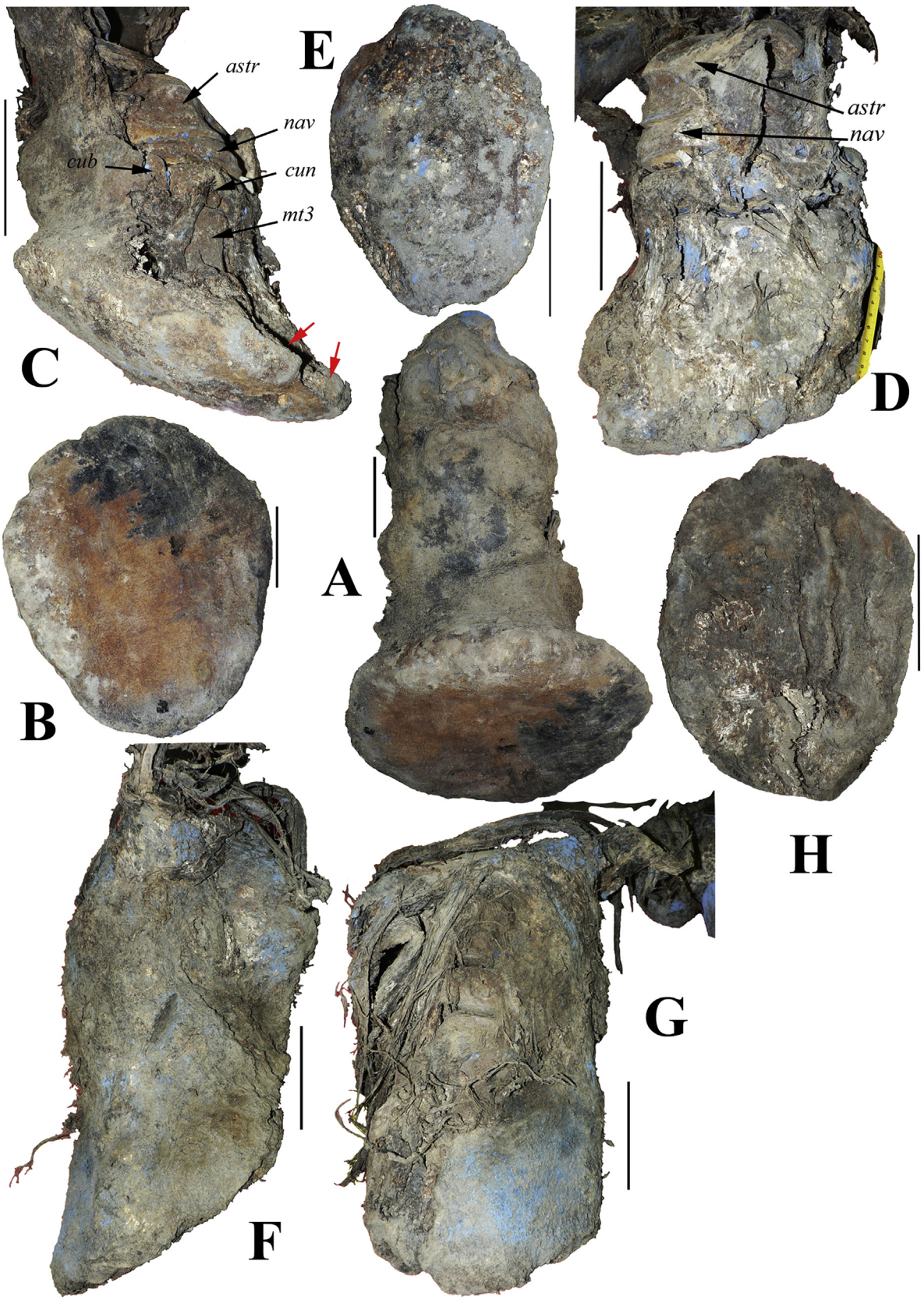

Fig. 21. The Zhenya Mammoth left forefoot (A, B) and right (C–E) and left (F–H) hind feet. A, G – frontal views; B, E, and H – plantar views; C, F – lateral views; D – medial view; ast – astragal, nav–navicular, cun – external cuneiform, mt3 – metatarsal 3. Scale 10 cm.

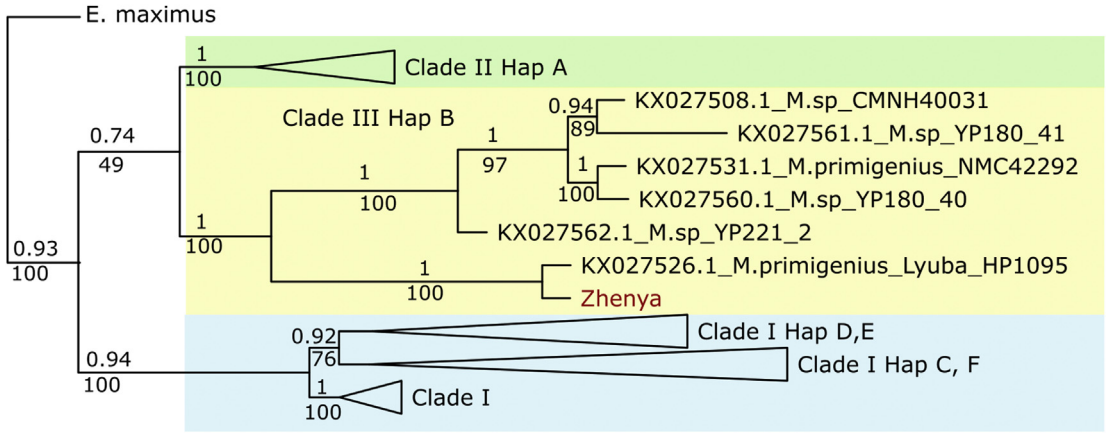

Fig. 22. The phylogenetic relationship of the Zhenya Mammoth mitochondrial genome and 102 previously published mammoth mitochondrial genomes. This is a consensus phylogeny based on Bayesian and Maximum Likelihood analyses, with major clades collapsed according to Enk et al. (2016). Node values are Bayesian posterior probabilities (above branch) and Maximum Likelihood bootstrap support (below branch). Detailed phylogenies with labeled tips are provided as supplementary Figs. S9 and 10.

than Zhenya's stature. The von Bertalanffy growth function of captive Asian elephant males 0–15 years of age ($H = 236[1-e^{(-0.182(t+4.82)}]$; Sukumar et al., 1988; Sukumar, 2003) predicts for 8 and 10 year old individuals the statures range between 213.11 and 220.10 cm, which are shorter (pSH 4.5%, or 10.8 cm) than Zhenya's height. Despite the extensive data collected for Asian elephants, it is highly likely that this function yields overestimated results due to oversize and overweight tendency of the captive animals (Larramendi, 2016), and should be used with caution.

It is also reasonable to presume that Zhenya's developmental rate was continuous from the first months of birth. This assumption is indirectly supported by the steadiest and fastest rates of body growth observed for modern elephants during their first 15 years (Sukumar et al., 1988; Lee and Moss, 1995; Shrader et al., 2006), a probable characteristic for most extinct taxa of Proboscidea. Zhenya's postnatal development rate after birth was higher than that in modern elephants. Study of the woolly mammoth babies from the Sevsk locality and the baby Lyuba's dental histology also showed high developmental rate in this species (Maschenko, 2002; Rountrey et al., 2012; Fisher et al., 2012).

4.3. Physiological condition

According to descriptions of the two types of fat found on other mammoth carcasses, distinguished by color, the distinctive yellow coloration of the Zhenya Mammoth fat found on the neck and along the spine indicate that it may be brown adipose tissue, or brown fat. Unlike the white fat, which stores energy, so-called “brown” fat is a derivative of skeletal muscle (Enerbäck, 2009) which evolved to protect animals from cold conditions. It serves as the energy reserve and insulation of the body: it is found in the neck and trunk of adult mammals, but is especially abundant in newborns and hibernating mammals (Himms-Hagen, 1990; Virtanen et al., 2009). This thermogenic process may be vital in neonates exposed to cold and unable to shiver, to keep them warm (Himms-Hagen, 1990). Indeed, the brown fat forming the visible neck hump was discovered in a very young baby mammoths, the calf Khroma (Maschenko, 2012) and the female baby Lyuba (Fisher et al., 2012).

Research on humans has shown that adults also have small and scattered pockets of brown fat spread around the body, predominantly in the neck and upper chest areas (Nedergaard et al., 2007). In a few studied mammal species, including humans, brown fat has been shown to be cold-induced and a metabolically significant tissue (Nedergaard et al., 2007). The retention of (or cold induced) brown fat was possibly the case for Zhenya and might have been common for young individuals of woolly mammoth, as a vital adaptation to survive in cold environment.

Thick layer of subcutaneous fat indicates that Zhenya was physiologically prepared for winter. A similar strategy of accumulation of large quantities of fat was observed in African elephants, when they prepare to survive the coming dry season, the hardest time of the year (Haynes, 1991).

4.4. Pathological changes

There were several types of developmental abnormalities found among Zhenya's bones, from lesions on several skeletal elements to underdeveloped teeth (upper M2s) and complete absence of teeth (lower m2s, left tusk), which are not characteristic for a normal pre-adolescent individual. We suspect that the absence of the left tusk and missing developing molars in the mandible were most likely caused by congenital disease. The bone lesions, some of which showed signs of successive healing according to descriptions in Krzemińska et al. (2015), were most likely signs of metabolic disorder causing physiological stress. The underdeveloped or missing teeth have not been previously recorded for the woolly mammoth.

The cranial and vertebral lesions similar to Zhenya's lesions were detected in other woolly mammoth specimens recovered from different European and Siberian sites, such as the Kraków Spadizta Street (B) Site (Poland), the Milovice I and Předmosti sites (Czech Republic), the Sevsk Site (Russia), and others (Maschenko et al., 2002, 2006; Wojtal and Sybczyk, 2005; Krzemińska, 2008, 2009; Krzemińska et al., 2015). These types of lesions were even reported for modern elephants (Haynes and Klimowicz, 2015). The young age of Zhenya confirms that similar type of bone disorders in the woolly mammoth were common in young and young adult individuals and were not only associated with old age (Wojtal and Sobczyk, 2005; Krzemińska and Wędzicha, 2015). The bone resorption forming different kind of lesions and bone deformation was also reported for modern and fossil Artiodactyla, Perissodactyla, and Proboscidea, diagnosed as signs of erosive arthritis, spondyloarthropathy, and/or tuberculosis (Rothchild, 2003; Rothchild et al., 2001, 2004; Rothchild and Martin, 2006).

4.5. Zhenya's bone modifications

The cranium, mandible, hyoid bones, and scapula that we examined had “dry” breaks typical for deteriorated bones and

indicative of post-mortem loss of moisture and organic content. All the cranial bones including the maxillae with "green" breaks on their ventral sides, had remained *in situ* in correct position in the cranium. All cranial parts had been supported by surrounding sediments until the whole skull was excavated, detached from the rest of the remains, and removed from the site. The *in situ* positions of the broken bones within the cranium would not be preserved if the cranium had been broken before it was buried. Among other bones with modifications, the fifth rib with deep cut mark made by a sharp edge appears to be the result of skinning and cleaning soft tissues from the carcass, and the second rib had a scratch left by a scoop or shovel used to remove sediments from the torso. Neither of these marks have solid evidence for being inflicted by prehistoric artifacts, as claimed by Pitulko et al. (2016). In addition to these "prehistoric cut marks", more preparator's marks made by sharp edges were found on bones (vertebrae) during the study of the skeleton (Fig. 1, H).

As for the tusk breakage, there is a substantial amount of evidence demonstrating similar patterns produced both by human activities and by elephants fighting (Khlopachev and Girya, 2010; Pitulko et al., 2015a, b; 2016; Haynes, 1991 and references therein). Therefore, identification of sources of such impacts would rely heavily on the context of such occurrences. Of major importance would be the presence of prehistoric artifacts or their debris (multiple flakes) at the ivory processing site, the presence of ivory or bone debris in proximity to archeological sites, and rationality and motivation reflected in prehistoric human knapping actions. However, the Zhenya mammoth site contained no lithic, bone, ivory, antler, or other artifacts. Another important clue about possible human use of the carcass would have been evidence of rational human behavior directed towards maximum utilization of natural resources, namely the meat and other raw materials that should have been harvested from the carcass, which did not take place. There is also no sufficient evidence indicatig that humans killed this mammoth as part of an "ivory industry," as it was proposed for the Yana site in eastern Siberia by Pitulko et al. (2015 a, b). The Zhenya's tusk remained in the cranium. The possibility that humans knapped the sub-vertically oriented tusk tip sticking out of the ground, in a very awkward position, and thus producing irregular flakes, seems irrational and nonfunctional, as does the proposed breaking of the facial part of the skull lying on its side. Paleolithic people left evidence at archeological sites that tusks could be removed from crania by cutting a deep circular groove at the alveoli's edge to loosen the tusk (Pitulko et al., 2015b, Fig. 17), but this was not observed on the Zhenya Mammoth cranium.

4.6. Zhenya's growth rate

The data on sizes above suggest that Zhenya either grew faster than modern elephants reaching its large size at the earlier age, or its rate of growth was similar with Recent elephants, but the teeth had delay in development. The rudimentary condition of second molars and absence of one tusk may seem to support the latter case, however, these features reflect the pathological state of the teeth, which would never develop further (M2/m2) or grow (left tusk) in Zhenya' life. While the reason for undeveloped left permanent tusk remains unclear, the undeveloped second lower molars and rudimentary upper second molars might have been caused by congenial disease or even cancer. Such undeveloped or underdeveloped molars have never been associated with developmental delay of the teeth erupted in front of them (Dunfee et al., 2006; Som and Curtin, 2003). The presence of normally developed D4/d4 and M1/m1 and development of one normally grown right tusk strongly indicate that Zhenya's rate of development (growth and tooth replacement) did not have delay and was normal until its death. At his age of 8–10 AEY, Zhenya reached live body size (pSH 227.4 cm) of some fully grown adult females of his species, indicating that his growth occurred at faster rate than that of the modern elephants. In its turn, the fast organismal development is a strong indicator of earlier onset of puberty and sexual maturity of the mammoth, which possibly were associated with stress and were reflected in additional "slow growth band" on his tusk (Fig. 10; C and D; see Section 3.3.3.1.4).

4.7. Zhenya's social status

It is known that the Asian elephants reach puberty around 8–15 years and are sexually mature in average at 10 years old, when the majority (99%) of the adolescent bulls (Subadult Class III, 10–15 years old) are normally expelled from the heard (Sukumar et al., 1988; Sukumar, 2003). Some 15 years old bulls of the Asian elephants were seen in musth (Sukumar, 1989). Based on Zhenya's size and age and indications of earlier onset of puberty and sexual maturity than in extant elephants, it is likely that Zhenya had been expelled from the herd relatively recently before death and was living as a single individual. The additional band B2 of early summer stress in the tusk deposited three years before Zhenya's death may reflect physiological stress caused by expelling Zhenya from the herd. The tusk's damage (shallow long grooves on the sides of the tusk tip) similar to those in African elephants (Fig. 11) indicates that Zhenya could have had first fights with other males, and even possibly had gone through his first musth.

4.8. Cause and season of death

The Zhenya carcass did not provide direct evidence that this mammmoth was killed by predators, modified by scavengers, or fell prey to prehistoric humans, and the site sediments give no indication that the mammoth was drowned in the river or a mud hole. The Zhenya's lack of one tusk was apparently more an inconvenience than a deadly danger, considering that wild Asian elephants with similar deviation of tusk development survive until old age (Eltringham, 1997). Despite the full hypoplasia of the left tusk and underdevelopment of the last unerupted molars, the teeth in wear were normal and functional, ruling out the possibility that these abnormalities could have been a direct cause of the mammoth's death. Similarly, few bone lesions and the development of the pain-free cysts inside the jaws could not have caused Zhenya's death. This mammoth also did not have any broken long bones, which is known to cause relatively quick death in modern African elephants (Haynes, 1991).

The presence of parasites such as nematodes in intestines is a common occurrence tolerated by Recent wild elephants, but animals suffer much more from parasites when they are stressed, especially youngsters (Sukumar, 2003). In extreme cases, helminthosis can cause animal deaths, but available data on the Zhenya Mammoth is not sufficient to make such a conclusion.

In modern elephants a few factors such as stress from being expelled from the heard, an animal's immaturity, and a lack of guidance from older individuals place young males at a higher mortality risk (Moss, 1996, 2000). Droughts bring additional stress to young African elephants, which are among the leading factors in mass deaths (Haynes, 1991). Starvation of youngest animals during drought periods is common, when exhausted elephants die by the waterholes. In the Arctic during the Late Pleistocene, the coldest seasons with freezing temperatures started earlier than today, drastically reducing water sources and increasing the drought period for woolly mammoths. At the end of arctic summer, lakes and small streams that froze early would mean the Yenisei River was the only available water refuge in the area, but not for long as it

too froze over. Limited open water sources would have attracted mammoths from far and near, and unrelated animals would have been aggressively competitive for access to water; males would have been especially aggressive and probably engaged in serious head to head fights, some of which may have resulted in injuries and deaths, as observed with Recent elephants (Haynes, 1991; Sukumar, 2003). Our analyses of the available data collected from the carcass indicate a strong possibility of behavior-related death resulting from Zhenya's involvement in a fight with a mature bull, damaging his single tusk, losing the battle, and dying from the acquired injury. Significant accumulation of subcuticular fat of the mammoth indicates that this battle might have happened between late summer and beginning of autumn, when the animal was in his best physiological condition before the hardest season of the year.

If Zhenya did not die under these circumstances, but survived, he would have faced death due to starvation at the age of 13–15 (± 1) AEY (age group X-XI; Laws, 1966), after wearing out his first (and last) normally developed molars (M1).

5. Conclusions

1. Zhenya Mammoth was an adolescent male 8–10 (± 1) AEY or somewhat older. Zhenya's estimated body weight was 2519 kg (including the hair).
2. The best estimate for Zhenya's physiological shoulder height (pSH) was 227.4 cm, which was similar to size of grown up females. This size indicates that Zhenya might have reached sexual maturity and was expelled from his herd living as a solitary individual.
3. Despite suffering from a congenital disease and missing one tusk, Zhenya developed at normal rate which was higher than in modern elephants.
4. The broken tusk shows that Zhenya might have participated in fight with other bull and was deadly injured.
5. Accumulation of large amounts of subcutaneous fat, morphology of the tusk, and preservation of the body in articulated condition indicates that Zhenya's died in Fall.
6. An analysis of ancient DNA provides strong support for Zhenya's mitochondrial lineage within the deeply diverging clade III haplogroup B.

Acknowledgments

This study was conducted within the 2013–2015 Program of Russian Academy of Science. The work of ENM, NVS, KKT and ANT was supported by the Program of the Presidium of Russian Academy of Sciences “Exploratory Fundamental Research for Development of the Russian Arctic”. IDS, AAV and GNO were supported by the grant of Russian Fund of Fundamental Studies "Ground Ice of the Western Arctic as a Data Archive of Global Environmental Changes” (16-05-00612) and partly funded by the government project "Changing the Earth's Cryosphere under the Influence of Natural and Technogenic Factors" (NIR AAAA-A16-116032810095-6). OP's studies in Zoological Institute (ZIN, St. Petersburg, Russia) and her travel was supported by the Mammoth Site of Hot Springs, SD. Inc. EP was supported by the 2016 Summer Research Grant from Bryn Athyn College (Philadelphia, PA). The authors thank all the personnel and organizations below, without whom this study would not have been possible. Mr. Alexey Bystrov ("Sopochnaya Karga" Meteorological Station) immediately reported on the find, and his staff and all the local residents enthusiastically assisted in the mammoth excavations. Dr. S. Rozhnov, Dr. A. Lopatin, Dr. P. Parkhaev and Dr. A. Rozanov (PIN) approved the proposal for funding the mammoth transportation and conservation by special Program of Russian Academy of Sciences. Mr. Gorbunov (International Mammoth Committee, Moscow, Russia), Ministry of Emergency Situations ((MES), Moscow), Administration of the Taimyr Regional Museum (Dudinka), and Zoological Institute, Russian Academy of Sciences, Russia, provided funds, logistics and direct assistance for the mammoth excavations, storage and transportation from the site to St. Petersburg, Russia. Dr. A.V. Lopatin (PIN), Sergei K. Shoigu (MES, Russian Geographical Society, Moscow), Vladimir A.Puchkov (MES, Moscow), Igor S. Buravchikov (MES, Krasnoyarsk), Evgeny I. Muraviev (“Norilskiy Nikel”, Norilsk), and Oleg I. Sheremetiev (Taimyr Administrative District of Krasnoyarsk Region, Krasnoyarsk) granted personal support in providing logistics and helicopter transportation of the mammoth on the route Sopochnaya Karga Cape – Dudinka – Norilsk, and cargo plane transportation Norilsk – Yaroslavl. Alla Pavlova (Taimyr Veterinary Laboratory, Dudinka) and Sergei V. Fedyaev (Station to Fight Animal Diseases, Dudinka) operatively conducted anthrax tests, which came out negative. Dr. Alexander Veselkin and Yu. Starikov (ZIN) arranged access to the mammoth carcass in ZIN, and Yuriy Starikov (ZIN) shared the photos and information on the Zhenya Mammoth's preparation and conservation. Dr. Gary Haynes generously shared his photos of the tusks' tips of the African elephants. Dr. Alexander Cherkinsky (Center for Applied Isotope Studies University of Georgia, Athens, GA) kindly suggested and performed the first radiocarbon analysis of the samples in 2012. Julia Mossman (Hot Springs, SD, USA) and Dr. Gary Haynes (University of Nevada, Reno) edited the manuscript. The authors express sincere gratitude to four anonymous reviewers for the comments, advices and editorial work, which significantly improved the manuscript. Finally, the authors thank the volume editor, Dr. A. Athanassiou for his constant support and tremendous interest to this paper.

All the authors have contributed to this paper: ENM and ANT prepared the proposal for funding by Russian Academy of Sciences; ANT excavated the mammoth; ENM, ANT, NVS and KKT provided logistics for the mammoth transportation from the field; IDS, AAV and GEO performed the field and lab work of the Zhenya Site deposits; IDS and OP wrote the text on geology; JvdP prepared the AMS dates and the relevant text; ENM and OP studied the mammoth; ENM wrote initial description of the Zhenya Mammoth in Russian and provided all Tables measurements and majority of the mammoth photos; EP and OP made calculations of allometric parameters; OP and EP wrote Sections 4.2 and 5; OP wrote Sections 3.3.3.1.4, 4.1, and 4.3–4.8, added Sections 2.1 and 2.2, prepared the final version of the manuscript in English, edited all the photos and prepared all the composite color Plates of the mammoth.

Appendix A. Supplementary data

Supplementary data related to this article can be found at http://dx.doi.org/10.1016/j.quaint.2017.06.055.

References

Aerts, A.T., van der Plicht, J., Meijer, H.A.J., 2001. Automatic AMS samplecombustion and CO_2 collection. Radiocarbon 43, 293–298.

Agenbroad, L.D., 1994. Taxonomy of north american *Mammuthus* and biometrics of the Hot springs mammoths. In: Agenbroad, L.D., Mead, J.I. (Eds.), The Hot Springs Mammoth Site: a Decade of Field and Laboratory Research in Paleontology, Geology, and Palaeoecology. Fenske Printing, Inc., Rapid City, SD, pp. 158–207.

Agenbroad, L.D., Mead, J.I., 1994. The taphonomy of *Mammuthus* remains in a closed system trap, Hot Springs Mammoth Site, South Dakota. In: Agenbroad, L.D., Mead, J.I. (Eds.), The Hot Springs Mammoth Site: a Decade of Field and Laboratory Research in Paleontology, Geology, and Palaeoecology. Fenske Printing, Inc., Rapid City, SD, pp. 283–305.

Astakhov, V.I., 2013. Pleistocene glaciations of northern Russia – a modern view. Boreas 42, 1–24.

Averianov, A.O., 1994. Mamont Kutomanova. Trudy Zoologicheskogo Instituta RAN

256, 111–134.
Averianov, A.O., 1996. Sexual dimorphism in the mammoth skull, teeth and long bones. In: Shoshani, J., Tassy, P. (Eds.), The Proboscidea: Evolution and Paleoecology of Elephants and Their Relatives, Oxford University Press, New York, NY, pp. 260–267.
Behrensmeyer, A.K., 1978. Taphonomic and ecologic information from bone weathering. Paleobiology 4 (2), 150–162.
Behrensmeyer, A.K., 1988. Vertebrate preservation in fluvial channels. Palaeogeogr. Palaeoclimatol. Paleoecol. 63, 183–199.
Behrensmeyer, A.K., Kidwell, S.M., Gastaldo, R.A., 2000. Taphonomy and paleobiology. Paleobiology 8 (3), 211–227.
Blumenbach, I.F., 1799. Handbuch der Naturgeschichte. Dieterich, Göttingen.
Boeskorov, G.G., Tikhonov, A.N., Lazarev, P.A., 2007. A new find of a mammoth calf. Dokl. Biol. Sci. 417, 480–483.
Boeskorov, G.G., Cherkashina, A.P., Belolyubskiy, I.N., Zaytsev, A.I., 2009. Osobennosti morfologii i paleoekologii Chekurovskogo mamonta. Otechestvennaya Geol. 5, 84–90 (in Russian).
Boeskorov, G., Potapova, O.R., Maschenko, E.M., Protopopov, A.V., Kuznetsova, T.V., Agenbroad, L., Tikhonov, A.N., 2014. Preliminary analyses of the frozen mummies of mammoth (*Mammuthus primigenius*), bison (*Bison priscus*) and horse (*Equus* sp.) from the Yana-Indigirka Lowland, Yakutia, Russia. Integr. Zool. 9, 471–480.
Boessenkool, S., Hanghøj, K., Nistelberger, H.M., Der Sarkissian, C., Gondek, A.T., Orlando, L., Barrett, J.H., Star, B., 2016. Combining bleach and mild pre-digestion improves ancient DNA recovery from bones. Mol. Ecol. Resour. http://dx.doi.org/10.1111/1755-0998.12623.
Campos, P.F., Gilbert, T.M.P., 2012. DNA extraction from keratin and chitin. In: Shapiro, B., Hofreiter, M. (Eds.), Ancient DNA: methods and Protocols, Methods in Molecular Biology 840. Humana Press, New York, NY, pp. 43–49.
Chaplin, R.E., 1971. The Study of Animal Bones from Archaeological Sites. Seminar Press, London and New York.
Christiansen, P., 2004. Body size in proboscideans, with notes on elephant metabolism. Zool. J. Linn. Soc. 140, 523–549.
Cuvier, G., 1799. Mémoire sur Les Espèces dÉléphant Vivantes et Fossiles. Mem. Inst. Natl. Sci. Arts Sci. Math. Phys. 2, 1–22.
Dabney, J., Knapp, M., Glocke, I., Gansauge, M.T., Weihmann, A., Nickel, B., Valsiosera, C., Carcía, N., Pääbo, S., Arsuaga, J.L., Meyer, M., 2013. Complete mitochondrial genome sequence of a Middle Pleistocene cave bear reconstructed from ultrashort DNA fragments. Proc. Nat. Acad. Sci. USA 110 (39), 5758–15763.
Darriba, D., Taboada, G.L., Doallo, R., Posada, D., 2012. jModelTest 2: more models, new heuristics and parallel computing. Nat. Methods 9 (8), 772.
Dubrovo, I., 1982. Morfologiya skeleta Yuribeiskogo Mamonta. In: Sokolov, V.E. (Ed.), Yuribeiski Mamont. Nauka, Moskva (in Russian).
Dunfee, B.L., Sakai, O., Pistey, R., Gohel, A., 2006. Radiologic and pathologic characteristics of benign and malignant lesions of the mandible. Radiographics 26 (6), 1751–1768.
Eales, N.B., 1926. The anatomy of the head of a foetal African elephant, *Elephas africanus* (*Loxodonta africana*). Trans. R. Soc. 54 (3), 491–551. Edinburgh.
Edgar, R.C., 2004. MUSCLE: multiple sequence alignment with high accuracy and high throughput. Nucl. Acids Res. 32 (5), 1792–1797. http://dx.doi.org/10.1093/nar/gkh340.
El Aldi, J.J., Cherney, M.D., Fisher, D.C., Harris, J.M., Farrell, A.B., Cox, S.M., 2015. Last years of life and season of death of a Columbian mammoth from Rancho La Brea. Nat. Hist. Mus. Los Angel. Cty. Sci. Ser. 42, 65–80.
Efremov, M.A., 1950. Tafonomiya i geologicheskaya letopis. Tr. Paleontol. Instituta 24, 1–179 (in Russian).
Eltringham, S.K., 1997. The Illustrated Encyclopedia of Elephants. From Their Origins and Evolution to Their Ceremonial and Working Relationship with Man. Salamander Books, London – N.Y.
Enk, J., Devault, A., Widga, C., Saunders, J., Szpak, P., Southon, J.R., Rouillard, J.-M., Shapiro, B., Golding, B., Zazula, G.D., Froese, D.G., Fisher, D., MacPhee, R.D., Poinar, H., 2016. Mammuthus population dynamics in Late Pleistocene North America: divergence, phylogeogrpaphy and introgression. Front. Ecol. Evol. 4 (00042), 1–13. http://dx.doi.org/10.3389/fevo.2016.00042.
Enerbäck, S., 2009. The origins of brown adipose tissue. N. Engl. J. Med. 360 (19), 2021–2023.
Fisher, D.C., Tikhonov, A.N., Kosintsev, P.A., Rountrey, A.N., Buigues, B., Plicht, J., 2012. Anatomy, death, and preservation of a woolly mammoth (*Mammuthus primigenius*) calf, Yamal Peninsula, northwest Siberia. Quat. Int. 255, 94–105.
Fisher, D.C., Shirley, E.A., Whalem, C.D., Calamari, Z.T., Rountrey, A.N., Tikhonov, A.N., Buigues, B., Lacombat, F., Grigoriev, S., Lazarev, P.A., 2014. X-ray computed tomography of two mammoth calf mummies. J. Paleobiology 88 (4), 664–675.
Garutt, V.E., Dubinin, V.E., 1951. O skelete Taimyrskogo mamonta. Zool. Zhurnal 30, 17–23 (in Russian).
Garutt, V.E., 1954. Yuzhnyi slon *Archidiskodon meridionalis* (Nesti) iz pliotsena severnogo poberezh'ya Azovskogo morya. Tr. Kom. po Iycheniu Chetvertichnogo Perioda (2), 1–76 (in Russian).
Garutt, V.E., 1964. Das Mammut, *Mammuthus primigeniius* (Blumenbach). A. Ziemsen Verlag, Wittenberg Lutherstadt.
Garutt, V.E., 2001. 200 let so vremeni ustanovleniya vida sherstistogo mamonta *Mammuthus primigeius* (Blumenbach, 1799). In: Rozanov, A.Yu (Ed.), Mamont I Ego *Okruzhenie*: 200 Let Izucheniya. GEOS, Moskva, pp. 7–21 (in Russian).
Garutt, V.E., Foronova, I.V., 1976. Issledovaniya Zubov Iskopayemykh Slonov: Metodologicheskiye Rekomendatsii. Vsesoyuznyy Institut Geologii, Geofiziki i Mineralogii, SO AN SSSR, Novosibirsk, pp. 1–36 (in Russian).
Garutt, V.E., Gentry, A., Lister, A.M., 1990. *Mammuthus* Brookes 1828 Mammalia Proboscidea proposed conservation and *Elephas primigenius* Blumenbach 1799 currently *Mammuthus primigenius* proposed designation as the type species of *Mammuthus* and designation of a neotype. Bulletin Zool. Nomencl. 47 (1), 38–44.
Glamazdin, I.G., Serduk, N.V., Panova, O., Maschenko, E.N., 2014a. Parazitologicheskiye issledovaniya organov i tkaney sopkarginskogo mamonta (*M. primigenius*) (Taimyr, Rossiya). In: Mater. Dokl. Nauchnoy Konf. Teoriya i Praktika Borby s Parazit. Boleznyami, Vypusk 15. Moskva, May 20-21st, 2014, pp. 74–77 in Russian.
Glamazdin, I., Panova, O., Serduk, N., Maschenko, E., 2014b. Preliminary results of parasitological research of a woolly mammoth, *Mammuthus primigenius* from Taimyr Peninsula, Russia. In: Abstracts of SVP 74th Annual Meeting, p. 139. November 5-8, 2014, Berlin.
Gusev, E.A., Arslanov, H.A., Maksimov, F.E., Molodkov, A.N., Kuznetsov, V.U., Smirnov, S.B., Chernov, S.B., Zherebtsov, I.E., Levchenko, S.B., 2011. Novye geochronologicheskie dannye po neopleistotsen-golotsenovym otlozheniyam nizoviev Eniseya. Probl. Arktiki I Antarkt. 2 (88), 36–44 (In Russian).
Gusev, E.A., Molodkov, A.N., Derevyanko, L.G., 2015. Sopkarginskyi Mamont, vremya i usloviya ego obitaniya (sever zapadnoi Sibiri). Uspekhi Sovrem. Estestvozn. (Geologo-Mineralogicheskie Nauki) 1, 432–435 (in Russian).
Guthrie, R.D., 1990. Frozen Fauna of the Mammoth Steppe: the Story of the Blue Babe. University of Chicago Press, Chicago & London.
Haynes, G., 1988. Spiral fractures, cutmarks and other myths about early bone assemblages. Nev. State Mus. Anthropol. Pap. 21, 145–151.
Haynes, G., 1991. Mammoths, Mastodonts and Elephants. Biology, Behavior, and Fossil Record. Cambridge University Press, Cambridge.
Haynes, H., 2017. Finding meaning in mammoth age profiles. Quat. Int. 443, (Part A), 65–78. http://dx.doi.org/10.1016/j.quaint.2016.04.012.
Haynes, G., Klimovicz, J., 2015. A preliminary review of bone and teeth abnormalities seen in recent *Loxodonta* and extinct *Mammuthus* and *Mammut*, and suggested implications. Quat. Int. 379, 1–12.
Hertz, O.F., 1902. Otchety nachal'nika ekspeditsii Imperatorskoy Akademii Nauk na Berezovku dlya raskopki trupa mamonta. Izv. Imperatorskoy Akad. Nauk. 26 (4), 11–174 (in Russian).
Himms-Hagen, J., 1990. Brown adipose tissue thermogenesis: interdisciplinary studies. FASEB J. 4 (11), 2890–2898.
Jónsson, H., Ginolhac, A., Schubert, M., Johnson, P.L.F., Orlando, L., 2013. mapDamage2.0: fast approximate Bayesian estimates of ancient DNA damage parameters. Bioinformatics 29, 1682–1684.
Kevrekidis, C., Mol, D., 2016. A new partial skeleton of *Elephas (Palaeoloxodon) antiquus* Falconer & Cautley, 1847 (Proboscidea, elephantidae) from Amynatio, Macedonia, Greece. Quat. Int. 406 (B), 35–56.
Kharlamova, A., Saveliev, S., Kurtova, A., Cherikov, V., Protopopov, A., Boeskorov, G., Plotnikov, V.V., Ushakov, V., Maschenko, E.N., 2016. Preserved brain of the woolly mammoth (*Mammuthus primigenius* (Blumenbach, 1799)) from the Yakutian permafrost. Quat. Int. 406 (B), 86–93.
Khlopachev, G.A., Girya, Ye.Yu., 2010. Sekrety Drevnikh Kostorezov Vostochnoy Yevropy I Sibiri. In: Priemy Obrabotki Bivnya Mamonta I Roga Severnogo Olenya v Kamennom Veke. Nauka, Sankt-Peterburg.
Kirillova, I.V., Shidlovskiy, F.K., Khasanov, B.F., 2011. First finding of a mammoth female (*Mammuthus primigenius* blum.) on the Taimyr Peninsula. Dokl. Earth Sci. 436 (2), 193–196.
Kirillova, I.V., Shidlovskiy, F.K., Titov, V.V., 2012. Kastatyakh Mammoth from Taimyr. Quat. Int. 276–277, 269–277.
Kosintsev, P.A., Laptev, E.G., Trofimova, S.S., Zanina, O.G., Tikhonov, A.N, Van der Plicht, J., 2012. Environmental reconstruction inferred from the intestinal contents of the Yamal baby mammoth Lyuba (*Mammuthus primigenius* Blumenbach, 1799). Quat. Int. 255, 231–238.
Krzemińska, A., 2008. Preliminary characteristics of pathologies found in the skeletons of mammoths at the Krakow Spadzista Street (B). Vterinarija Ir. Zootech. 43 (65), 52–57.
Krzemińska, A., 2009. Pathologies of mammoth bones from Milovice site. In: Oliva, M. (Ed.), Milovice: Site of the Mammoth People below the Pavlov Hills, Studies in Anthropology, Paleoethnology and Quaternary Geology, 27(19), pp. 118–125.
Krzemińska, A., Wędzicha, S., 2015. Pathological changes on the ribs of woolly mammoths (*Mammuthus primigenius*). Quat. Int. 359–360, 186–194.
Krzemińska, A., Wojtal, P., Oliva, M., 2015. Pathological changes on woolly mammoth (*Mammuthus primigenius*) bones: holes, hollows and other minor changes in the spinous processes of vertebrae. Quat. Int. 359–360, 178–185.
Kuzmina, I.E., 1999. Morfometricheskoe opisanie skeleta. Trudy Zoologicheskogo instituta SSSR 275, 32–38 (in Russian).
Larramendi, A., 2016. Shoulder height, body mass, and shape of proboscideans. Acta Paleontol. Pol. 61 (3), 537–574.
Laws, R.M., 1966. Age criteria for the African elephant *Loxodonta africana*. East Afr. Wildl. J. 4, 1–37.
Lazarev, P.A., 2002. Kadastr Mestonakhozhdeniy Fauny Mlekopitayushchikh Pozdnego Kaynozoya Yakutii. Moskva, Novosibirsk (in Russian).
Lazarev, P.A., 1980. Krupnyye Mlekopitayushchiye Antropogena Yakutii. Nauka, Novosibirsk (in Russian).
Lee, P.C., Moss, C.J., 1995. Statural growth in known-age African elephants. J. Zool. 236, 29–41.
Leschinskiy, S.V., 2012. Paleoecological investigation of mammoth remains from the

Kraków Spadzista street. Quat. Int. 276–277, 155–169.
Li, H., Durbin, R., 2009. Fast and accurate short read alignment with Burrows-Wheeler transform. Bioinformatics 25. http://dx.doi.org/10.1093/bioinformatics/btp324.
Lister, A.M., 1999. Epiphyseal fusion and postcranial age determination in the woolly mammoth *Mammuthus primigenius*. Deinsea 6, 79–87.
Lister, A.M., Stuart, A.J., 2010. The West Runton mammoth (*Mammuthus trogontherii*) and its evolutionary significance. Quat. Int. 228, 180–209.
Lomakin, V.V., 1948. Dinamicheskiye fazy rechnykh dolin i allyuvial'nykh otlozheniy. Zemlevedeniye 2 (42), 154–187 (in Russian).
Longin, R., 1971. New method of collagen extraction for radiocarbon dating. Nature 230, 241–242.
Maglio, V.J., 1973. Origin and evolution of the elephantidae. *Transactions of the American Philosophical Society*. New Ser. 63, 1–149.
Maschenko, E.N., 2002. Individual development, biology and evolution of the woolly mammoth *Mammuthus primigenius* (Blumenbach, 1799). Cranium 19 (1), 1–120.
Maschenko, E.N., Gablina, S.S., Tesakov, A.S., Simakova, A.N., 2006. The Sevsk woolly mammoth (*Mammuthus primigenius*) site in Russia: taphonomic, biological, and bahavorial interpretations. Quat. Int. 142–143, 147–165.
Maschenko, E.M., 2012. Osobennosti detenysha mammonta (*Mammuthus primigenius*) s reki Khroma. Zool. Zhurnal 91 (9), 1124–1140 (in Russian).
Maschenko, E.N., Potapova, O., Boeskorov, G., Plotnikov, V., Agenbroad, L., 2012. Preliminary data on the new partial carcass of the woolly mammoth, *Mammuthus primigenius*, from Yakutia, Russia. In: Abstracts of Papers 72nd Annual SVP Meeting, p. 137. October 17-20, Raleigh, NC.
Maschenko, E., Potapova, O., Tikhonov, A., 2014a. A crippled young woolly mammoth (*Mammuthus primigenius*), from the Taimyr Peninsula, Russia: new data on the ontogenetic development of the species. In: Abstracts of Papers 74th SVP Annual Meeting, p. 181. November 5-8, 2014, Berlin.
Maschenko, E., Tikhonov, A., Serdyuk, N., Tarasenko, K., Cherkinsky, A., Gorbunov, S., van der Plicht, J., 2014b. The partial carcass of the mammoth "Zhenya" (*Mammuthus primigenius*) from western Taimyr Peninsula, Russia: preliminary analysis and results. In: Proceedings of the VIth International Conference on Mammoths and Their Relatives. Scientific Annals, vol. 101. School of Geology, Aristotle University, Thessaloniki, Greece, pp. 121–122.
Maschenko, E.N., Tikhonov, A.N., Serduk, N.V., Tarasenko, K.K., Lopatin, A.V., 2015. A finding of a male mammoth carcass in the Karginsky suit of the Upper Pleistocene of the Taimyr Peninsula. Dokl. Biol. Sci. 460, 32–35.
Maschenko, E., Boeskorov, G.G., Baranov, A.V., 2013. Morphology of a mammoth calf (*Mammuthus primigenius*) from Ol'chan (Oimiakon, Yakutia). Paleontological J. Mosc. 4, 74–88.
McGowan, G., Prangnell, J., 2006. The significance of vivianite in archaeological settings. Geoarcheology 21 (1), 93–111.
Meyer, M., Kircher, M., 2010. Illumina sequencing library preparation for highly multiplexed target capture and sequencing. Cold Spring Harbor Protoc. http://dx.doi.org/10.1101/pdb.prot5448.
Mol, D., Ligtermoet, L.J., 1985. Over het tongbeen van de mammoet en vondsten hiervan in gewande en Heerewaarden. Cranium 2 (2), 16–21.
Mol, D., Tikhonov, A., van der Plicht, J., Kahlke, R.-D., Debruyne, R., Geel, B., Reenen, G., Pals, J.P., Marliave, C., Reumer, J.W.F., 2006. Results of the CERPOLEX/*Mammuthus* expeditions on the Taimyr Peninsula, arctic Siberia, Russian Federation. Quat. Int. 142–143, 186–202.
Molodkov, A., Bolikhovskaya, N., 2009. Climate change dynamics in Northern Eurasia over the last 200 ka: evidence from mollusc-based ESR-chronostratigraphy and vegetation successions of the loess–palaeosol records. Quat. Int. 201, 67–76.
Mook, W.G., 2006. Introduction to Isotope Hydrology: Stable and Radioactive Isotopes of Hydrogen, Oxygen and Carbon. Taylor and Francis, London.
Mook, W.G., Streurman, H.J., 1983. Physical and chemical aspects of radiocarbon dating. In: First Symposium on ^{14}C and Archaeology, Groningen. PACT 8, pp. 31–55.
Moss, C., 1996. Getting to know a population. Studying elephants. In: Kangwana, K. (Ed.), Studying Elephants, vol. 7. AWF Technical handbook series, Nairobi, pp. 58–74.
Moss, C., 2000. Elephant Memories: Thirteen Years in the Life of an Elephant Family. University of Chicago Press, Chicago, 364 pp.
Nedergaard, J., Bengtsson, T., Cannon, B., 2007. Unexpected evidence for active brown adipose tissue in adult humans. Am. J. Physiol. (Endocrinol. Metab.) 293, E444–E452.
Nikolsky, P., Pitulko, V., 2013. Evidence from the Yana Palaeolithic site, Arctic Siberia, yields clues to the riddle of mammoth hunting. J. Archeol. Sci. 40 (12), 4189–4197.
Oblogov, G.E., 2015. Evolyutsiya Kriolitozony Poberezh'ya Karskogo Morya V Pozdnem Neopleystotsene – Golotsene. In: Diss. Na Soiskaniye Uchenoy Stepeni Kandidata Geologo-mineralogicheskikh Nauk. Institut Kriosfery Zemli, Tyumen, 197 pp. (in Russian).
Osborn, H.F., 1942. Proboscidea, vol. 2. American Museum of Natural History, New York.
Palkopoulou, E., Mallick, S., Skoglund, P., Enk, J., Rohland, N., Li, H., Omrak, A., Vartanyan, S., Poinar, H., Götherström, A., Reich, D., Dalén, L., 2015. Complete genomes reveal signatures of demographic and genetic declines in the woolly mammoth. Current Biol. 25 (10), 1395–1400. http://dx.doi.org/10.1016/j.cub.2015.04.007.
Pilgram, T., Western, D., 1986. Inferring the sex and age of African elephants from tusk measurements. Biol. Conserv. 36, 39–52.
Pitulko, V.V., Pavlova, E.Yu, Nikolskiy, P.A., 2015a. Obrabotka bivnya mamonta v verkhnem paleolite Arkticheskoy Sibiri (po materialam Yanskoy stoyanki). Strat. Plus 1, 223–283 (in Russian).
Pitulko, V.V., Pavlova, E.Yu, Nikolskiy, P.A., 2015b. Mammoth ivory technologies in the Upper Paleolithic: a case study based on the materials from Yana RHS, northern Yana-Indigirka lowland, Arctic Siberia. World Archeol. 47 (3), 29–57.
Pitulko, V.V., Tikhonov, A.N., Pavlova, E.Y., Nikolsky, P.A., Kuper, K.E., Polozov, R.N., 2016. Early human presence in the Arctic: evidence from 45,000-year-old mammoth remains. Science 351 (6270), 260–263.
Reimer, P.J., Bard, E., Bayliss, A., Beck, J.W., Blackwell, P.G., Ramsey, C.B., Buck, C.E., Edwards, R.L., Friedrich, M., Grootes, P.M., Guilderson, T.P., Haflidason, H., Hajdas, I., Hatté, C., Heaton, T.J., Hoffmann, D.L., Hogg, A.G., Hughen, K.A., Kaiser, K.F., Kromer, B., Manning, C.W., Niu, M., Reimer, R.W., Richards, D.A., Scott, E.M., Southon, J.R., Staff, R.A., Turney, C.S.M., van der Plicht, J., 2013. IntCal13 and Marine13 Radiocarbon age calibration curves 0-50,000 years cal BP. Radiocarbon 55, 1869–1887.
Romanenko, F.A., Kanevskiy, M.Z., Streletskaya, I.D., Vasil'yev, A.A., Gusev, YeA., Vanshteyn, B.G., Nikolayev, V.I., 2005. Novyye dannyye o stroyenii chetvertichnykh otlozheniy vostochnogo berega Yeniseyskogo zaliva. In: Abstracts Mezhd. Konf. Prioritetnyye Napravleniya V Izuchenii Kriosfery Zemli. *Pushchino*, pp. 176–177. Pushchino, (in Russian).
Ronquist, F., Huelsenbeck, J.P., 2003. MRBAYES 3: Bayesian phylogenetic inference under mixed models. Bioinformatics 19, 1572–1574.
Roth, V.L., 1990. Estimates of body size for insular dwarf mammoths. In: Damuth, J.D., MacFadde, B.J. (Eds.), Body Size in Mammalian Paleobiology: Estimation and Biological Implications, 1990. Cambridge University Press, Cambridge, pp. 151–180.
Roth, V.L., Shoshani, J., 1988. Dental identification and age determination in *Elephas maximus*. J. Zool. 214, 567–588.
Rothchild, B.M., 2003. Pathology in Hiscock site vertebrates, and its bearing on hyperdisease among north American mastodons. In: Laub, R.S. (Ed.), The Hiscock Site: Late Pleistocene and Holocene Paleoecology and Archeology of Western New York State. Bull. of Buffalo Society of Natural Sciences, vol. 37, pp. 171–175.
Rothchild, B.M., Martin, L.D., 2006. Skeletal impact of disease. N. M. Mus. Nat. Hist. Bull. 33, 1–226.
Rothchild, B.M., Prothero, D.R., Roschild, C., 2001. Origins and spondyloarthropathy in Perissodactyla. Clin. Exp. Reumatology 19, 628–632.
Rothchild, B.M., Wang, X., Shoshani, J., 2004. Spondyloarthropathy in proboscideans. J. Zoo Wildl. Med. 25 (3), 360–366.
Rothe, M., Kleeberg, A., Hupfer, M., 2016. The occurrence, identification and environmental relevance of vivianite in waterlogged soils and aquatic sediments. Earth-Science 158, 51–64.
Rountrey, A.N.D., Fisher, D.C., Tikhonov, A.N., Kosintsev, P.A., Lazarev, P.A., Boeskorov, G., Buigues, B., 2012. Early tooth development, gestation, and season of birth in mammoths. Quat. Int. 255, 196–205.
Shapiro, B., Hofreiter, M., 2012. Ancient DNA: Methods and Protocols. Humana Press, 247 pp.
Shoshani, J., Eisenberg, J., 1982. *Elephas maximus*. Mamm. Species 182, 1–8.
Shoshani, J., 2003. *Mammut* hyoid elements from the Hiscock site: description and implications. In: Laub, R.S. (Ed.), The Hiscock Site: Late Pleistocene and Holocene Paleoecology and Archeology of Western New York State. Bulletin of the Buffalo Society of Natural Sciences, vol. 37, pp. 114–120.
Shrader, A.M., Ferreira, S.M., McElveen, M.E., Lee, P., Moss, S., van Aarde, R.J., 2006. Growth and age determination of African savanna elephants. J. Zool. 270, 40–48.
Smith, K.M., Fisher, D.C., 2011. Sexual dimorphism of structures showing indeterminate growth: tusks of American mastodons (*Mammut americanum*). Paleobiology 37 (2), 175–194.
Smith, K.M., Fisher, D.C., 2013. Sexual dimorphism and inter-generic variation in Proboscidean tusks: multivariate assessment of American mastodonts (*Mammut americanum*) and extant African Elephants. J. Mammal Evol. 20 (4), 337–355.
Sokolov, V.Ye, Sumina, Ye.B., 1982. Morfologiya volosyanogo pokrova mamontenka. In: Verschagin, N.K., Mikhelson, V.M. (Eds.), Magadanskii Mamontenok 81–84 (in Russian).
Som, P.M., Curtin, H.D., 2003. Head and Neck Imaging. Mosby, St. Louis.
Stamatakis, A., 2014. RAxML version 8: a tool for phylogenetic analysis and post-analysis of large phylogenies. Bioinformatics 30 (9), 1312–1313. http://dx.doi.org/10.1093/bioinformatics/btu033.
Starikov, YuV., Petrova, E.A., 2016. Sopkarginskiy Mamont: Izgotovleniye Kompleksa Muzeynykh Eksponatov. In: Abstracts Bioraznoobraziye Prirodnykh Sistem: Biologicheskiye Resursy Rossii: Otsenka Sostoyaniya I Fundamental'nyye Osnovy Monitoringa. Zoologicheskii Institut RAN, St. Petersburg, pp. 35–37 (in Russian).
Streletskaya, I.D., Surkov, A.V., Semenov, S.V., 2005. Issledovaniye Chetvertichnykh Otlozheniy Rossiyskogo Severa Metodom Granulo-mineralogicheskogo Analiza (P-ov Yamal, Ust'ye R. Yenisey). In: Materialy IV Vserossiyskogo Soveshchaniya Po Izucheniyu Chetvertichnogo Perioda "Kvarter-2005". Geoprint, Syktyvkar, pp. 405–407 (in Russian).
Streletskaya, I.D., Vasiliev, A.A., Kanevski, M.Z., Vanshtein, B.G., Shirokov, R.S., 2006. Organicheskiy uglerod v chetvertichnykh otlozheniyakh poberezhya karskogo morya. Kriosf. Zemli 10 (4), 35–43 (in Russian).
Streletskaya, I.D., Gusev, E.A., Vasiliev, A.A., Kanevski, M.Z., Anikina, N.U.,

Derevyanko, L.G., 2007. Novye resultaty kompleksnykh issledovaniy chetvertichnykh otlozheniy zapadnogo Taimyra. Kriosf. Zemli 11 (3), 14–28 (in Russian).
Streletskaya, I.D., Vasiliev, A.A., Kanevskiy, M.Z., 2008. Freezing of marine sediments and formation of continental permafrost at the coasts of Yenisey Gulf. In: Proceedings of 9th International Conference on Permafrost, vol. 2. Institute of Northern Engineering, University of Alaska, Fairbanks, Alaska, pp. 1721–1726.
Streletskaya, I.D., Vasiliev, A.A., Gusev, YeA., Kanevskiy, M.Z., Medvedev, M.A., Vanshteyn, B.G., Cherkashev, G.A., Bol'shiyanov, D.Y.U., 2009. Chetvertichnyye otlozheniya, podzemnyye l'dy, i dinamika beregov Zapadnogo Taimyra. In: Kassens, A.P., Lisitsyn, Y. Tide, Polyakova, Yel., Timokhov, L.A., Frolov, I.Ye (Eds.), Sistema Morya Laptevykh I Prilegayushchikh Morey Arktiki. Sovremennoye Sostoyaniye i Istoriya Razvitiya, Moskva, MGU, pp. 357–372 (in Russian).
Streletskaya, I.D., Vasiliev, A.A., Meyer, H., 2011. Isotopic composition of syngenetic ice wedges and paleoclimatic reconstructions, Western Taimyr, Russian Arctic. Permafr. Periglac. Process. 22 (1), 101–106.
Streletskaya, I.D., Gusev, E.A., Vasiliev, A.A., Oblogov, G.E., Anikina, N.U., Arslanov, H.A., Derevyanko, L.G., Pushina, Z.V., 2013a. Geologicheskoye stroyeniye chetvertichnykh otlozheniy beregov zapadnogo Taimyra. Kriosf. Zemli 17 (3), 17–26 (in Russian).
Streletskaya, I.D., Gusev, E.A., Vasiliev, A.A., Oblogov, G.E., Molodkov, A.N., 2013b. Plestocene-Holocene paleoenvironmental records from permafrost sequences at the Kara Sea coast (NW Siberia, Russia). Geography. Environ. Sustain. 3 (6), 60–75.
Streletskaya, I.D., Vasiliev, A.A., Melnikov, V.P., Oblogov, G.E., 2014. Estimation of atmospheric paleo-circulation based on isotope composition of ice wedges. Dokl. Earth Sci. 457 (2), 1025–1027.
Sukumar, R., Joshi, N.V., Krishnamurthy, 1988. Growth in the Asian elephant. Proc. Indian Acad. Sci. 97, 561–571.
Sukumar, R., 1989. The Asian Elephant. Ecology and Management. Cambridge University Press, Cambridge.
Sukumar, P., 2003. The Living Elephants, Evolutionary Ecology, Behavior, and Conservation. Oxford University Press, Oxford.
Tolmachoff, I.P., 1929. The carcass of the mammoth and rhinoceros found in the frozen ground of Siberia. Trans. Am. Philosophical Soc. 22 (1), 11–74.
Van den Merwe, N.J., Bezuidenhout, A.J., Seegers, C.D., 1995. The skull and mandible of the African elephant (*Loxodonta africana*). Onderstepoort J. Veterenary Res. 62, 245–260.
van der Plicht, J., Wijma, S., Aerts, A.T., Pertuisot, M.H., Meijer, H.A.J., 2000. The Groningen AMS facility: status report. Nucl. Instrum. Methods B 172, 58–65.
van der Plicht, J., Palstra, S.W.L., 2016. Radiocarbon and mammoth bones: what's in a date. Quat. Int. 406, 246–251.
van Geel, B., Fisher, D., Rountrey, A.N., van Arkel, J., Duivenvoorden, J.F., Nieman, A.M., van Reenen, G.B.A., Tikhonov, A.N., Buigues, B., Gravendeel, B., 2011. Palaeo-environmental and dietary analyses of intestinal contents of a mammoth calf (Yamal Peninsula, northwest Siberia). Quat. Sci. Rev. 30, 3935–3946.
Vereshchagin, N.K., 1977. Berelekhskoye 'kladbishche' Mamontov. Trudy Zool. Inst. AN SSSR 72, 5–50 (in Russian).
Vereschagin, N.K., 1981. Morfometricheskoe opisanie mamontenka. In: Vereschagin, N.K., Mikhelson, V.M. (Eds.), Magadanskii Mamontenok. Nauka, Leningrad, pp. 52–80.
Vereshchagin, N.K., 1999. Yamal'skiy Mamontenok: Morfometricheskoye Opisaniye Skeleta. Trudy Zool. Inst. RAS 275, 32–38 (in Russian).
Vereshchagin, N.K., Tikhonov, A.N., 1986. Issledovaniye Bivney Mamontov. Trudy Zoologicheskogo instituta AN USSR 149, 3–14 (in Russian).
Vereshchagin, N.K., Tikhonov, A.N., 1999. Exterior of the mammoth. Cranium 16, 4–44.
Virtanen, K.A., Lidell, M.E., Orava, J., Heglind, M., Westergren, R., Niemi, T., Taitotten, M., Laine, J., Savitso, N.J., Enerback, S., Nuutila, P., 2009. Functional brown adipose tissue in healthy adults. N. Engl. J. Med. 360 (15), 1518–1525.
Vollosovich, K.A., 1914. Mamont s ostrova Bol'shogo Lyakhovskogo (Novosibirskiye ostrova). Geologicheskiy ocherk. Zap. Imperatorskogo Mineral. Obschestva 2 (50), 305–338 (in Russian).
Wheatley, B.P., 2008. Perimortem or postmortem bone fractures? An experimental study of fracture patterns in deer femora. J. Forensic Sci. 53 (1), 69–72.
White, P.A., Diedrich, C.G., 2012. Taphonomy story of a modern African elephant *Loxodonta africana* carcass on a lakeshore in Zambia (Africa). Quat. Int. 276–277, 287–296.
Wojtal, P., Sobczyk, K., 2005. Man and woolly mammoth at the Kraków Spadzista Street (B) – taphonomy of the site. J. Archeol. Sci. 32, 193–206.
Zalenskii, V.V., 1903. Osteologicheskiya i odonlologicheskiya issledovaniya nad mamontom (*Elephas primigenius Blum.*) i slonami (*El. Indicus* L. and *El. Africanus* Blum.). In: Nauchnye rezultaty ekspeditsii snaryazhennoi imperatorskoi akademiei nauk dlya raskopki mamonta. Naidennogo na Reke Berezovke V. 1901 gody 1, pp. 1–124 (in Russian).
Zaslavskiy, M.A., 1971. Novyi Metod Izgotovleniya Chuchel Zhivotnykh: Skul'pturnaya Taksidermiya. Nauka, Moskva-Leningrad.